Modeling and Analysis of Microgrid Energy Management System and Control of Standalone Photovoltaic System:

(Case Study Ambo University Information Center Technology Building)

Paulos Geremew Feyisa

A Thesis Submitted to

The Department of Electrical Power and Control Engineering

School of Electrical Engineering and Computing

Presented in Partial Fulfillment of the Requirement for the Degree of Master's in

Electrical Power and Control Engineering (Power Engineering)

Office of Graduate Studies

Adama Science and Technology University

August, 2021

Adama, Ethiopia

Modeling and Analysis of Microgrid Energy Management System and Control of Standalone Photovoltaic System:
(Case Study Ambo University Information Center Technology Building)

Paulos Geremew Feyisa
Advisor: Molla Biweta (Ph.D.)

A Thesis Submitted to
The Department of Electrical Power and Control Engineering
School of Electrical Engineering and Computing

Presented in Partial Fulfillment of the Requirement for the Degree of Master's in
Electrical Power and Control Engineering (Power Engineering)

Office of Graduate Studies
Adama Science and Technology University

August, 2021
Adama, Ethiopia

DECLARATION

I hereby declare that this Master Thesis entitled "Modeling and Analysis of Microgrid Energy Management System and Control of Standalone Photovoltaic System: (A case study of Ambo University Information Center Technology Building)" is my original work. That is, it has not been submitted for the award of any academic degree, diploma, or certificate in any other university. All sources of materials that are used for this thesis have been duly acknowledged through citation

Paulos Geremew Feyisa ________	____________________	__________________
Name of Student	Signature	Date

RECOMMENDATION

I, the advisor of this thesis, hereby certify that I have read the revised version of the thesis entitled "Modeling and Analysis of Microgrid Energy Management System and Control of Standalone Photovoltaic System: (A case Study of Ambo University Information Center Technology Building)" prepared under my guidance by **Paulos Geremew** submitted in partial fulfillment of the requirements for the degree of Masters of Science in Electrical Power and Control Engineering (Power). Therefore, I recommend the submission of revised version of the thesis to the department following the applicable procedures.

Dr. Molla Biweta ______________	__________________	________________
Advisor	Signature	Date

APPROVAL SHEET

I, the advisor of the thesis entitled "Modeling and Analysis of Microgrid Energy Management System and Control of Standalone Photovoltaic System: (A case study of Ambo University Information Center Technology Building)" and developed by **Paulos Geremew Feyisa**, hereby certify that the recommendation and suggestions made by the board of examiners are appropriately incorporated into the final version of the thesis.

Dr. Molla Biweta	____________________	__________________
Advisor	Signature	Date

We, the undersigned, members of the board of examiners of the thesis by **Paulos Geremew** have read and evaluated the thesis entitled "Modeling and Analysis of Microgrid Energy Management System and Control of Standalone Photovoltaic System: (A case study of Ambo University Information Center Technology Building)" and examined the candidate during the open defense. This is, therefore, to certify that the thesis is for partial fulfillment of the requirement of the degree of Master of Science in Electrical Power and Control Engineering (Power).

________________________________	____________________	__________________
Chairperson	Signature	Date
________________________________	____________________	__________________
Internal Examiner	Signature	Date
________________________________	____________________	__________________
External Examiner	Signature	Date

Finally, approval and acceptance of the thesis is contingent upon submission of its final copy to the Office of Postgraduate Studies (OPGS) through the Department Graduate Council (DGC) and School Graduate Committee (SGC).

________________________________	____________________	__________________
Department Head	Signature	Date
________________________________	____________________	__________________
School Dean	Signature	Date
________________________________	____________________	__________________
Office of Postgraduate Studies, Dean	Signature	Date

ACKNOWLEDGEMENTS

First of all, I want to thank God Almighty. I am proud to thank all the excellent and talented people who helped me complete this paper. Next, I sincerely thank and deeply thank my research advisor, **Dr. Molla Biweta**, for his friendly manners, guidance and inspiration in the research process and courses, as well as all emails, meetings, suggestions, suggestions and many good ideas exchanges.

I am particularly grateful to **Dr. Tefera Terefe** for his support, patience, and helpful attitude throughout my thesis work. I would like to thank the department Postgraduate Coordinator **Dr. Milkias Berhanu** for providing their all support. Finally, I must express my gratitude to my parents. Especially, my uncle **Professor Getahun Merga** and my brother **Mr. Tamirat Geremew** for their continuous encouragement and support throughout my study period.

TABLE OF CONTENTS

LIST OF TABLES

LIST OF FIGURES

LIST OF ACRONYMS

AC	Alternating Current
BDC	Bidirectional Converter
BMS	Battery Management System
COE	Cost Of Energy
CRF	Capital Recovery Factor
DC	Direct Current
DER	Distributed Energy Resources
DOD	Depth Of Discharge
EEU	Ethiopian Electric Utility
EMS	Energy Management System
FF	Fill Factor
FLC	Fuzzy Logic Controller
HOMER	Hybrid optimization model for Renewable Energy
IC	Incremental Conductance
ICT	Information Centre Technology
IGBT	Insulated Gate Bipolar Transistor
KW	Kilowatt
LCOE	Levelized Cost of Energy
MATLAB	Matrix Laboratory
MPPT	Maximum Power Point Tracker
NASA	National Aeronautics and Space Administration
O&M	Operation and Maintenance
PG	Power Generation
PID	Proportional Integral Derivative
PL	Power Load
P&O	Perturb and Observe
PV	Photovoltaic
PWM	Pulse Width Modulation
SOC	State of Charge
STC	Standard Test Condition
TNPC	Total Net Present Cost

LIST OF SYMBOLS

a	Diode ideality factor
d	Discount rate
E_{pv}	Total energy required from the PV array
G	Actual irradiance in W/m^2
i	Inflation rate
I_d	Diode saturation current,
I_{pv}	Light generated current of the photovoltaic cell
I_{scn}	Short-circuit current at the nominal condition
K	Boltzmann constant (1.38×10^{-23}) JK^{-1}
K_d	Derivative gain
K_i	Integral gain
K_p	Proportional gain
n	Lifetime in years
N_p	Number of cells connected in parallel
N_s	Number of cells connected in series
N_t	Total number of modules
P_{bat}	Battery power delivered to the load
P_{pv}	Total power of PV array in watts
q	Electronic charge (1.602×10^{-19})
Q_c	Remain capacity of the battery (Ah)
Q_r	Rated capacity of the battery (Ah)
R_p	Shunt resistance (Ω)
R_s	Series resistance (Ω)
T	Module operating temperature in Kelvin
ΔT	Deviation from the nominal temperature in Kelvin
V_d	The voltage across the diode:
V_{ocn}	Open-circuit voltage at the nominal condition

ABSTRACT

In recent years, the demand for electricity has been increasing every day, and microgrids have received more and more attention due to efficient and reliable power sources. Due to power fluctuations in power transmission systems, power distribution systems, power quality disturbances, and severe power outages that may cause significant changes in grid voltage and frequency, power systems are facing increasing challenges, and they make the system unstable. Therefore, this unstable power system is leads to insufficient power access, and making it difficult to achieve service continuity, which is more common in Ambo University information center technology. That is why the energy management system of the microgrid and the control of the standalone photovoltaic system are needed. The components used in the microgrid system were such as the maximum power point tracking, photovoltaic panels, batteries, and bi-directional DC to DC converters, and inverters were discussed. Data like solar energy resource, load demand, and weather conditions of the selected area was collected from primary and secondary resources. The energy demand of the selected site is 198.16 kWh. Based on the community's energy demand, CSS-MSP-250W photovoltaic panels, 12V, 200Ah deep cycle batteries were selected. In addition, the cost of the equipment used in the microgrid system is estimated and analyzed. The microgrid system is controlled using a fuzzy logic controller and a proportional, integral, and derivative (PID) controller is employed and analyzed to control the imbalance and variation of energy, to stabilize the DC link voltage at 400V, manage the battery, and fluctuation of power among the microgrid energy management system were proposed in this thesis work. Generally, the microgrid energy management system is efficient, reliable and balanced.

Keywords: *Battery, Converter, Fuzzy logic controller, Maximum power point tracking, Microgrid, off-grid, and Photovoltaic*

CHAPTER ONE

INTRODUCTION

1.1. Background

Currently, renewable energy is becoming an essential part of life. However, most of the people in developing countries are living without access to electricity. Especially, Ethiopia is one of these developing countries, which have no sufficient power supply [1].

The fact is that the demand for energy is growing day by day. Urbanization and industrialization have created a huge demand for energy or electricity [1]. Today, the global energy industry has entered a new era called "smart energy", which uses efficient, reliable, more sustainable, continuous and safe energy production/transmission/distribution system. The microgrid is a partial component of the load and the power, it operates in two modes in the mode connected to the network and disconnected mode or in the off-grid mode with the traditional centralized network (microgrid), and works in an autonomous. It is integrated with distributed energy sources (DER), such as renewable energy, solar energy storage systems or batteries.

Microgrids, smart grids and smart homes are the main technological importance in the field of smart energy today and in the future. Among these microgrid concepts, the energy management system (EMS) is explained in the following sections of this paper. Now, at this time, mainly in developed and developing countries, microgrids are being applied and used in university campuses, residential areas, industrial parks, farms and military camps. This research focuses on an off-grid microgrid energy management system, that can provide reliable and high-quality energy for all communities in the information center and technology building.

Due to the increasing demand for energy and the increase in global greenhouse gas emissions and air pollution, the microgrid system has been questioned [2]. Microgrid is a small power system composed of many distributed power generation equipment, which can meet the basic foundation of local demand, reduce customer power outage costs, system losses, and improve the level of renewable energy.

Also, the significant environmental changes are considered in the design of energy production and use of photovoltaic (PV) systems. However, energy is directly dependent on the environment, for example, due to changes in sunlight and temperature, the radiation in the photovoltaic system will change [3]. The standalone photovoltaic system consists of a photovoltaic system with MPPT, a bidirectional DC-DC converter, a controller, a battery, and an inverter. Due to the increase of power sources in the power system, microgrids have received more attention. In addition, it also utilizes renewable energy by optimizing the total cost of energy and stabilizing energy [4]. Generally, the energy management of microgrids is more efficient, saving energy by eliminating energy surplus and insufficiency.

The photovoltaic system is a solid semiconductor that depends mainly on the technology, which converts the fraction of the incident solar radiation (photons) from the DC electricity with empty emission of carbon. The photovoltaic system can provide electrical energy to an electrical grid that supplies electric power to a particular device and connected to an electrical network or a system outside the network.

There are two types of batteries: primary batteries or dry batteries and secondary batteries or rechargeable batteries. Primary batteries are stored and provide electricity, but they cannot be recharged. But secondary batteries can store and transport electrical energy, and can further charge and select solar photovoltaic systems.

In addition, the battery of the solar cell system has many advantages, such as energy storage capacity, voltage, current stabilization and autonomy. It stores electric power and then accumulates to supply power to the electrical charge according to the necessary requirements.

Charge controller is the basic requirement of photovoltaic system. The wires and cables come from solar panels and batteries, and all loads pass through the charge controller [5]. The function of the charge controller is to prevent the battery from charging, control how the photovoltaic panel charges the battery, send information about the change of the charge controller, protect the battery from being discharged, and disconnect the load when the battery voltage is too low. Also, due to changes in temperature and irradiance, the photovoltaic modules will also change.

This means that when the amount of solar radiation changes, the temperature of the photovoltaic energy will change, the output of the photovoltaic voltage, and current will also change [6]. Therefore, to control this change, the MPPT control will extract the maximum power from the photovoltaic module, according to the operating mode of the photovoltaic module.

1.2. Statement of the Problem

Ethiopia has abundant and reliable renewable energy resources. Today, energy demand is increasing day by day and global greenhouse gas emissions are constantly increasing; Due to the power transmission infrastructure, power distribution system power fluctuations, power quality disturbances and severe power outages, the power system is facing increasing challenges. Therefore, power fluctuations can cause significant changes in voltage and frequency, which can make the system unstable.

This unstable power system is leads to insufficient power access, especially which is more common in the Ambo University ICT center, and they are using the diesel or fuel generators, which is expensive. Instead of diesel or fuel, the use of photovoltaic solar energy is particularly important. Almost the communities do not have sufficient access to energy and it is difficult to achieve continuity of service. Therefore, to solve these problems, a standalone microgrid system is adopted to alleviate (reduce) power fluctuations, improve power quality, and bring reliability and higher efficiency to the system.

This problem is more common in the Ambo University information center technology building and can be overcome by reducing the total cost of energy and meeting the needs of the community. Therefore, it can be solved by adopting microgrid energy management system and standalone photovoltaic system control.

1.3. Objectives

1.3.1. General Objective

The main objective of this thesis is to develop and analysis the microgrid energy management system using maximum power point tracker, fuzzy and fuzzy-PID controller.

1.3.2. Specific Objectives

The specific objectives are to:

- Determine the power and energy demand of ICT center building Ambo University, Ethiopia.
- Estimate and select the size of the PV panel, battery, MPPT controller, and inverter.
- Model and analysis of microgrid energy management system using MATLAB/Simulink software
- Develop a control system using fuzzy-PID controller
- Optimize the microgrid energy management of the system using HOMER PRO software

1.4. Scope of the Study

The scope of this thesis work tried to evaluate renewable energy issues and challenges in access to electricity of ICT- center building Ambo University, Western Ethiopia, and also to modeling and analysis of the Microgrid energy management and control of standalone PV system for the selected area based on their energy demand.

1.5. Significance of the Study

Due to the application of modeling and analysis of energy management and control in microgrids, the results of the work of this thesis are useful for the ICT centers by providing uninterrupted and high-efficiency energy, as well as for users get more reliable, power balanced, and responding to demand by applying standalone photovoltaic system. Also, the work in this thesis will help other areas with similar insufficient electric access.

1.6. Limitations of the Study

In this thesis work, the simulation of system is limited to MATLAB/Simulink, and HOMER PRO software. Also, it is focused only on simulation rather than actual implementation, because it requires additional time, and cost to implement.

1.7. Organization of the Thesis

The organization structure of this paper is as follows:

Chapter one: This chapter includes introduction, background, problem statement and objective. It also contains the scope and limitations of this research.

Chapter two: Contains literature review. This chapter reviews related papers, journals and articles, and discusses most of the theoretical knowledge of the topic of this thesis.

Chapter three: This chapter uses a different methodology. In addition, the necessary data required for this study is described. All mathematical equations, procedures and calculations are also described. In addition, this chapter also includes, standalone photovoltaic system control and microgrid power management models in MATLAB/Simulink. Each component has a control model for system operation strategy.

Chapter four: This chapter presents the results and discussion. This chapter deals with the results obtained from the technical and economic analysis and modeling of the microgrid system.

Finally, in chapter five, an overall system conclusion, recommendations, and future works related to this study were stated.

CHAPTER TWO

LITERATURE REVIEW

2.1. Theoretical Background of Microgrid Energy

Microgrid is a small power system close to consumers. The microgrid system is usually described as a medium and low voltage distribution network containing several generations of power sources, controllable loads, and storage devices or batteries [7]. It especially plays a very important role in the use of renewable energy sources such as photovoltaic arrays.

After years of development, the microgrid concept and its technology have fully exploited, its benefits by providing optimized integration of renewable energy, saving energy costs and improving reliability. Similarly, microgrid applications have evolved into commercial and industrial systems with reliable power. The microgrid application is the embodiment of the smart grid concept. The smart grid concept describes the integration of technologies, equipment and systems that provide and use digital information and control to optimize energy efficiency, communication, reliability, security and protection [8]. Additionally, the microgrid provides flexibility and increased reliability for power system protection and control.

Microgrids are used to meet the energy needs of universities, hospitals, factories, data centers, military bases, or entire communities [2], [3]. The following Figure 2.1 shows the structure of the microgrid.

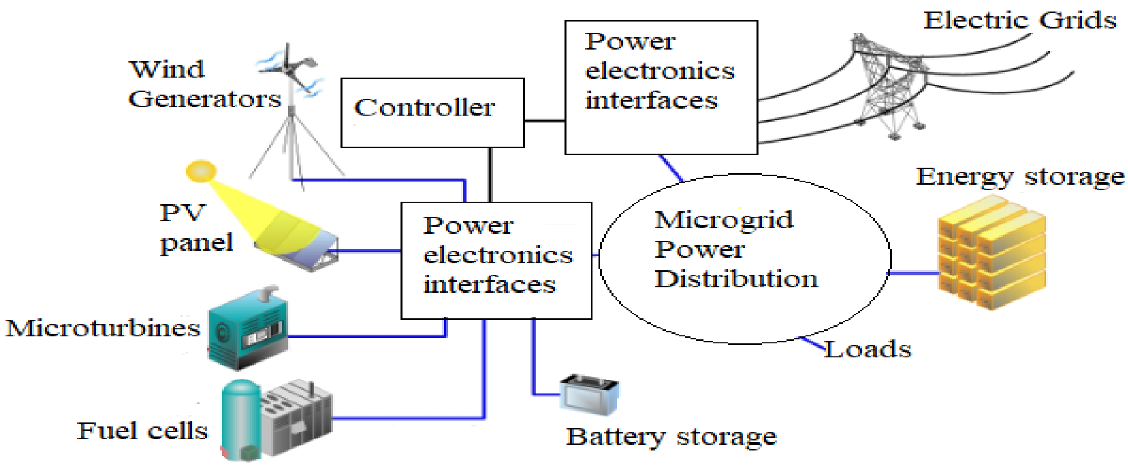

Figure 2.1. Structure of microgrid [11].

2.1.1 Types of Microgrid

i. Institutional microgrid: The campus environment or institutional microgrid consists of several buildings; they are electrically connected through the campus network. In addition, this type of microgrid is fully interconnected with public service networks and exists in the near era, with various loads.

ii. Remote "off-grid" microgrid: The remote or off-grid microgrid is an inherent area, far from any transmission, so it has nothing to do with the utility network.

iii. Commercial and industrial microgrids: This type of microgrid is more developed in Asia Pacific and North America [11]. But in the work of this thesis, an independent or off-grid microgrid system is proposed.

2.1.2. Microgrid Operation Mode

The microgrid can operate in two modes, which are defined as follows [12].

i. Standalone Mode: It is suitable for situations where the network is far away, the upstream network is faulty, or some maintenance operations are being performed.

ii. Grid-connected Mode: In this mode, the microgrid system is connected to the upstream network or public network. The microgrid can be partially powered or supplied from the main utility grid (depending on electricity or power exchange). But in this paper, an autonomous mode is proposed.

2.1.3. Control of Microgrid

The important unit that controls the operation of the microgrid is the microgrid management system, which operates independently or autonomously in the system, and connected to the network, applies bidirectional power exchange and supports the components of the microgrid system [8].

The microgrid energy management system is divided into three controls, which comprehensively manage the operation of the microgrid and maintain the balance between power generation and users [8], [13]. Such as primary control, secondary control and tertiary control, respectively, are introduced as follows:

i. Primary Control: The main control works within a range of multiple times or the fastest response time. The main control functions include off-grid detection, equalization control, converter output control, and voltage regulation.

ii. Secondary Control: It is the core layer for reliable and economical operation of the microgrid system. The secondary control functions as a power management and power generation control system. The power management system then minimizes the operating cost of the microgrid and improves its reliability. It also adjusts the energy flow of the microgrid system considering the state of charge of the energy storage system or the battery to ensure its normal operation and save the life cycle of the battery.

iii. Tertiary Control: It is the highest control and maintains the intelligence of the entire system or the entire microgrid system. It involves the energy market and organizes energy producers from an economic point of view considering the balance between consumers and energy generation [14]. Figure 2.2 below is the microgrid management system.

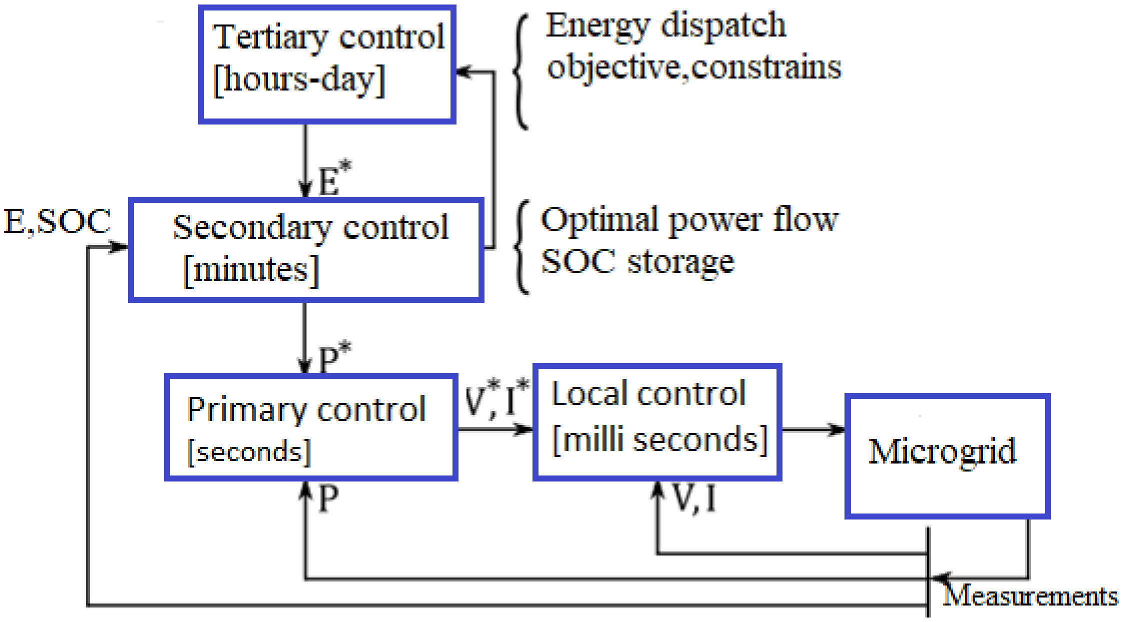

Figure 2.2. Microgrid energy management systems [14].

Advantages and disadvantages of using microgrid

The increase in energy demand has led to the use of microgrid, which has the following advantages for electric energy: Best environmentally, energy quality, operation and cost saving, and economy [15], [16]. In addition, in the microgrid, there are two ways to save costs: one is to use surplus energy and power operation mode, because the power source is close to the user's load, no energy or necessary infrastructure for energy is required. Second, cost savings is achieve by integrating the power generation system.

Generally, the advantages of microgrid are:

- More efficient
- More flexible
- Best environmentally friendly
- More modular
- Less vulnerable
- Easier to control.

However, with the advantages of microgrids, there are also some difficulties to deal with, such as high distributed energy load, high installation or investment costs, these difficulties can be encouraged by customers and the government.

2.1.4. Microgrid Components

i. Background of Photovoltaic System

The photovoltaic system is an attractive renewable energy source for distributed power generation due to its quiet operation and relatively small size [11]. As a result, photovoltaic energy has increased significantly across the world. Photovoltaic array generates energy, when exposed to sunlight [6]. However, multiple interface components are required to convert, control, distribute, conduct, and store the energy obtained by the photovoltaic array. The structures of PV are:

a. PV array: It is used to describe a group of modules in a single system. When the power generated by the module is not enough to meet certain applications, the modules can be connected in parallel, in series or meet the required power rating. Photovoltaic arrays consist of multiple modules and modules made up of cells. It is a complete power generation unit, containing any number of PV panels and modules.

b. PV cell: The photovoltaic cell is covered with a protective layer and becomes a photovoltaic module, which is the basic assembly block of the photovoltaic system. When light hits the surface of a solar cell, the solar cell accumulates semiconductors, so electrons are released and collected from the metal connected to the cell.

c. PV module: Cell combinations are called photovoltaic modules or called photovoltaic panels. Most of the time cells are connected in series to increase the voltage rating of the photovoltaic module or the panel. The electric power generated by the cell is very small.

Therefore, many cells are connected in series to increase the power rating. Figure 2.3 shows the photovoltaic structure of photovoltaic cells, modules and array.

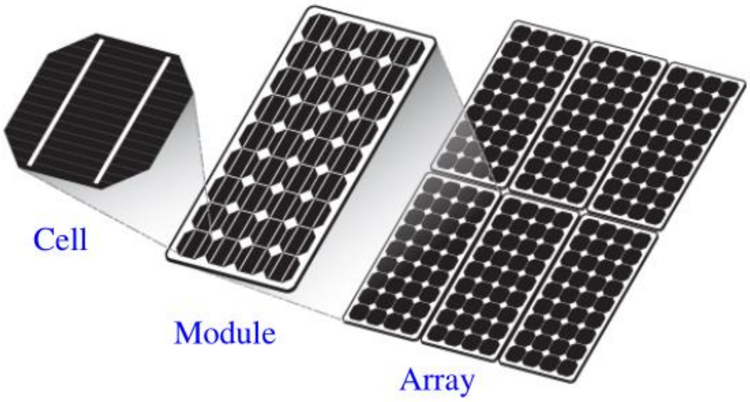

Figure 2.3. Structure of PV cell, module, and array [4].

ii. Types of Solar Photovoltaic Cells

Photovoltaic cells are manufactured in different ways using different materials. The material used for the structure of solar panels is silicon with semiconductor properties. The types of photovoltaic cells that dominate the world market fall into three categories:

- Monocrystalline silicon cell
- Polycrystalline silicon cell
- Thin film

a. Monocrystalline silicon photovoltaic cell

Monocrystalline silicon cells have high efficiency and strong heat resistance. However, their manufacturing process is low and labor intensive, making them more expensive than polycrystalline or thin films.

b. Polycrystalline silicon photovoltaic cell

Polycrystalline photovoltaic cells contain many small crystal grains instead of a single similar crystal structure. It is cheaper than monocrystalline cells, but has lower efficiency. Approximately 70% of the world's photovoltaic production is dominated by the world market.

c. Thin film

Nevertheless, crystalline photovoltaic cells still dominate the market, and these cells are also made of thin films. This makes them more durable and more flexible [17]. The result is very thin and flexible, and it uses less than 1% of the silicon required for a crystalline cell.

Due to the reduction of raw materials and lower energy manufacturing processes, the production cost of amorphous silicon cells is very low. Since the order of silicon atoms is smaller than that of crystals, the efficiency is greatly reduced.

Figure 2.4. Types of solar photovoltaic cells [17].

Table 2.1. Multi-criteria for types of photovoltaic cells [5].

Types of cells	Efficiency rate	Advantage	Disadvantage
Monocrystalline cell	20%	Highly efficient, Durable	Most expensive
Polycrystalline cell	15%	Less expensive, improving efficiency	Slightly lower efficiency not as durable
Thin film (Amorphous cell)	7- 10%	Low cost, easily Produced	Shorter warranties, shorter lifespan

iii. Working Principles of Solar Photovoltaic

Conversion of the light comes from into electricity, or which generates voltage or current is called the photovoltaic effect. When the semiconductor material in the photovoltaic cell is doped, a photovoltaic effect PN structure is formed. Positive or p-type silicon can give up electrons and gain holes, while n-type silicon accepts electrons.

When cells are affected by sunlight, photons from the light excite some electrons in the semiconductor to form negative-positive pairs or electron holes, and then form an electric field. This formed field causes positively charged particles to move in different direction. Free electrons tend to pass through the n-side rather than the p-side, because electrons move to the n-side, forming holes. Then the hole moves to the side or in the opposite direction to the electron. Through the movement of electrons, an electric current is formed in the cell. This process is called the way photovoltaic energy works in solar cells [19]. Figure 2.5 below shows the working principle of photovoltaic solar energy.

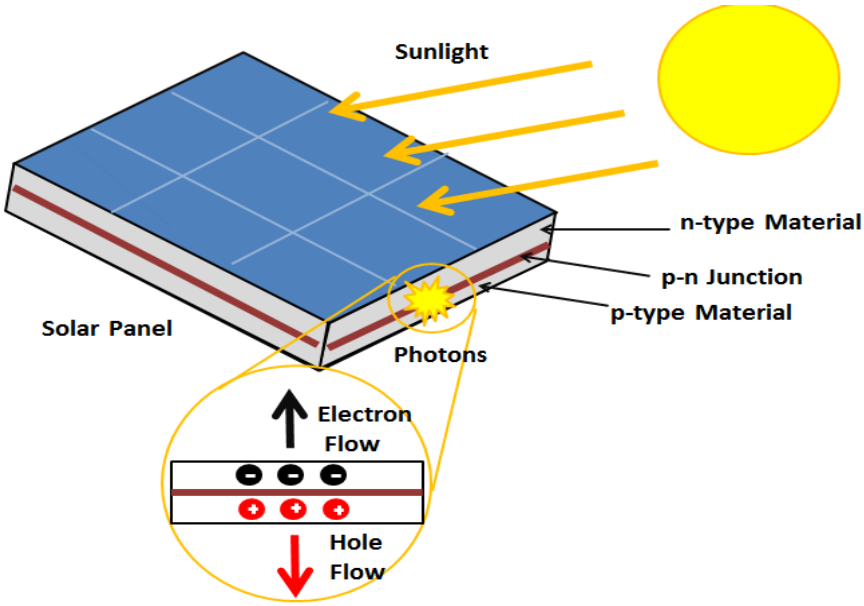

Figure 2.5. How photovoltaic solar works [19].

2.1.5. Electrical Characteristics of Photovoltaic Panel

Most PV modules are classified using standard test conditions (STC) [20]. Standard test conditions are defined as a set of laboratory test conditions that are similar to the conditions under which photovoltaic panels can be used.

Standard test conditions have the following factors:

Irradiance: It is the power or intensity of sunlight, described in watts per square meter falling on a flat surface. The measurement standard is expressed in 1000 watts per square meter.

Cell temperature: It will be different from the ambient air temperature. The standard test condition defines the battery test temperature as 25 ° C.

Advantages and disadvantages of photovoltaic modules:

Advantages: [6].

- ❖ The photovoltaic system is silent and visually discreet
- ❖ The energy produced by solar cells is silent and clean.
- ❖ Photovoltaic solar energy is a locally available renewable energy source.
- ❖ The photovoltaic system can be built in any size according to the energy demand.

Disadvantages:

- ❖ Photovoltaic solar energy is a variable energy source, due to temperature and irradiance.
- ❖ In addition, some toxic chemicals such as arsenic and cadmium are used in the photovoltaic production process.
- ❖ Photovoltaic panels are poorly maintained, easily damaged, and fragile.

2.1.6. Factors that Affect Reliability and Performance of PV Cell

i. Solar cell conversion efficiency (η)

The efficiency of photovoltaic solar cells is the relationship between the maximum output power produced and the incident or input power [22]. Some output parameters will affect the efficiency of photovoltaic solar cells, which are defined as follows.

$$\eta = \frac{V_{oc} \times I_{sc} \times FF}{P_{in}} \tag{2.1}$$

where: V_{oc} is open circuit voltage, I_{sc} is short circuit current, P_{in} is the incident light power on the device, and FF is the fill factor.

ii. Short circuit current

The short-circuit current is the current encountered, when the positive and negative electrodes of the cell are short-circuited; in addition, the voltage between the negative and positive terminals is zero, which corresponds to zero load resistance [22]. It depends on the spectrum of incident light and the density of incident photon flux.

iii. Open circuit voltage

It is the maximum voltage, when no current flows through the external circuit. Under open circuit voltage, the terminals of the photovoltaic solar cell are open or disconnected from the load.

iv. Fill factor

Fill factor is one of the important parameters to identify the efficiency of photovoltaic solar modules. In order to provide maximum efficiency, the fill factor should be the largest and close to unity on the current and voltage curves of the solar PV module. However, the value of the FF gives a concept of the quality of the photovoltaic array, the closer to unity, the greater the power that the array can provide [23]. It is the relationship between theoretical power and maximum power, expressed mathematically as follows. The IV curve of the solar cell variable fill factor is shown in Figure 2.6.

$$FF = \frac{V_{mp}\ I_{mp}}{V_{oc}\ I_{sc}} \tag{2.2}$$

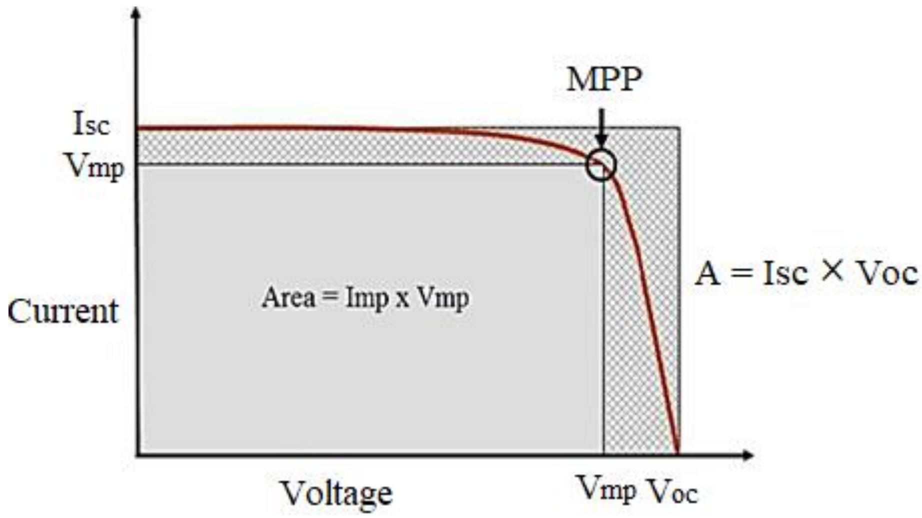

Figure 2.6. I-V Curve with a varying fill factor of solar cell [22].

2.1.7. Maximum Power Point Tracker

The maximum power point tracker is used to extract the maximum power from photovoltaic modules or panels under different irradiance and temperatures. The point where the photovoltaic module produces the maximum power is called the maximum power point.

The output characteristics of photovoltaic arrays are affected by changes in temperature and irradiance. When temperature and irradiance change, photovoltaic modules may not work at the maximum power point [24], [25]. Therefore, in order to overcome this problem, this paper chooses the P and O methods. It is a maximum power point tracking technology, which can extract maximum power from photovoltaic modules at any time and provide solar energy efficiency.

The induced power output in a photovoltaic module depends on the temperature and irradiance of the solar cell [26]. The photovoltaic module has a single operating point that can provide maximum energy to the load. This point is called the maximum power point, and it varies nonlinearly with cell temperature and solar irradiance, as shown in Figure 2.7.

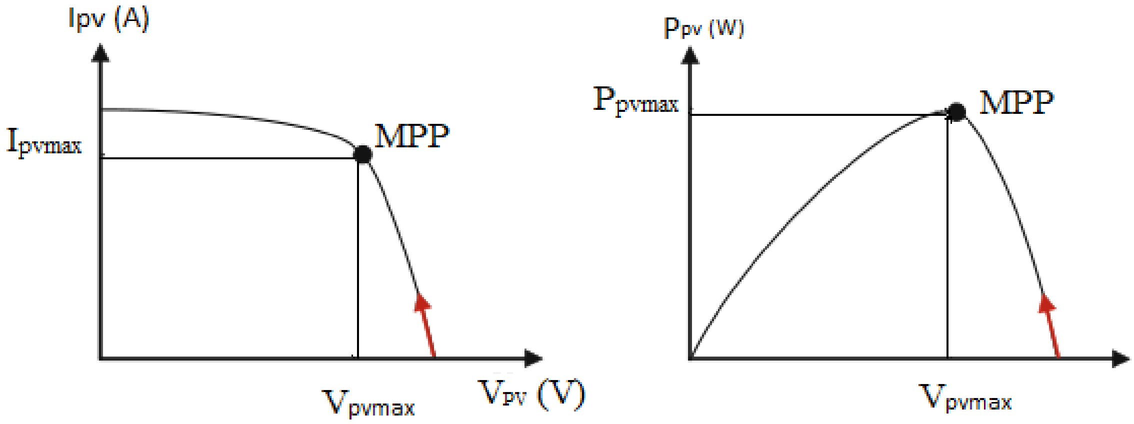

Figure 2.7. Maximum power points of I -V and P -V curves [7].

2.1.8. Perturb and Observe Technique

This technique is the simplest method. The time complexity of perturbation and observation methods is much lower. It will not stop at the maximum power point, but will continue to perturb in both directions. Once this happens, the algorithm is very close to MPP, and appropriate error limits can be set, or it can use a wait function, which will eventually increase the time complexity of the method.

The principle of the perturbation and observation algorithm is that with a small increase in the working voltage of the photovoltaic panel, it is perturbed. If the power change generated by the power supply is positive, it should go in the direction of MPP, and then continue to perturb in the same direction [27]. If the power change is negative, it will move away from the direction of the MPP, and the provided perturbation sign must be changed.

In this method, the first condition to check is that the current power is the same as the previous reading. If the power does not change, it should run at the inflection point of the

PV curve without changing the operating voltage. The second conditional statement compares the power of the previous value with the current value. The voltage is then compared with the previous value, and the direction of the maximum power point can be determined from these samples. The duty cycle is perturbed in the direction of power increase [28]. This method continues its working voltage from the photovoltaic module until the maximum power is obtained. The flow chart of the perturbation and observation method is shown in Figure 2.8 below.

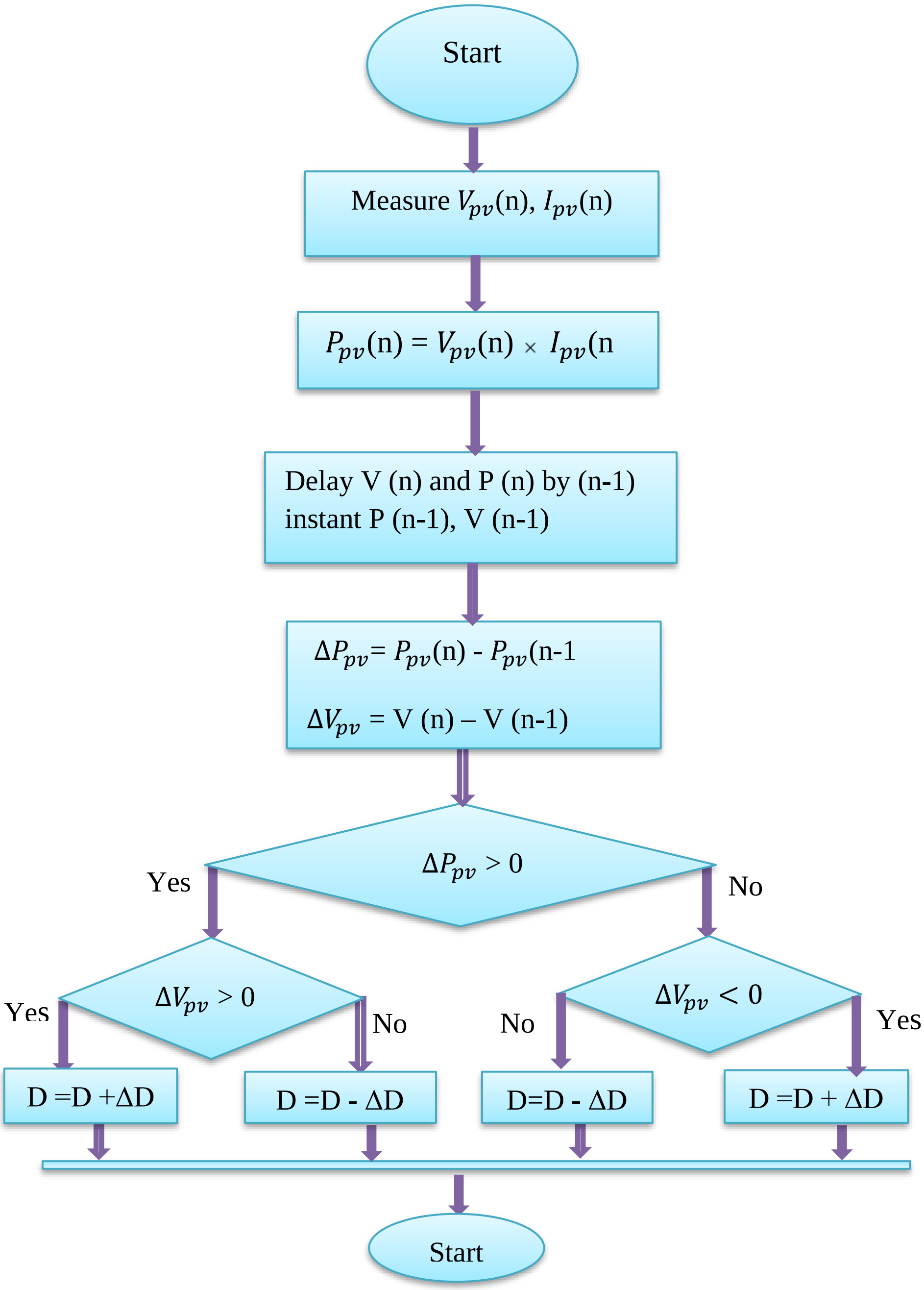

Figure 2.8. The flow chart of perturb and observe method [29].

2.1.9. DC to DC Converters

A DC to DC converter is a power electronic circuit that converts DC voltage from one level to another. There are many conversion methods, such as linear, electronic, magnetic, switch mode, and capacitance. Among them, the circuit described in this paper is a switch-mode DC to DC converter. This is an electronic device used, whenever there is a need to change DC power from one voltage level to another.

They basically just change the input power at various impedance levels [29]. There are various converters that can be used to change the voltage level to another level. Some of them are discussed below.

i. The buck converter
ii. The boost converter
iii. The buck-boost converter

i. The buck converter

A buck converter is used in a circuit that reduces the voltage level of the output voltage according to its requirements. The operation of a buck converter starts with an open switch, which means that no current flows anywhere in the circuit. When the switch is closed, the current flows through the inductor, which is slow at first, but gradually accumulates over time. When the switch is closed, the inductor draws current through the diode, which means that the voltage at the output of the inductor is lower than the first one.

ii. The Boost converter

A boost converter is a power converter whose output DC voltage is greater than its input DC voltage. This converter has the same components as the buck converter, but produces an output voltage greater than the source voltage.

iii. **Buck-boost converter**

Another basic switch-mode converter is the buck-boost converter [29]. The output of this buck-boost converter will be lower or higher than the input voltage.

2.1.10. Energy Storage System

Energy storage systems are key components used in microgrids that rely on renewable energy sources. It will provide voltage stability and smooth fluctuations that occur in renewable energy power generation [24].

The energy storage system is a backup system that integrates with the photovoltaic array through a bidirectional converter to provide reliability and energy stability by charging during off-peak load and discharge during peak load conditions. The energy generated by renewable energy has certain fluctuations [30].

Energy storage systems allow energy to be used, when there is not enough power to generate energy. The efficiency of the energy storage system will affect the performance of the system, so it is necessary to conduct deep study on energy storage [31]. There are different types of energy storage systems, such as batteries, fuel cells, flywheels, compressed air, and super capacitors. Among them, the battery is selected and discussed.

2.1.11. Battery

A battery is an electrochemical device that can directly convert the chemical energy contained in its active material into electrical energy, and vice versa [32]. Batteries are mainly used as storage elements, because they store energy through an electrochemical process and have a fast response during both discharging and charging. In addition, compared with other energy storage devices such as supercapacitors, fuel cells, compressed air systems, and flywheels, batteries have higher energy density. In addition, they can provide flexible power management to improve the power quality of the microgrid power generation system. [6]. Generally, batteries can be divided into two categories: primary batteries and secondary batteries.

i. Primary batteries: These batteries are not rechargeable and cannot be charged, once expelled and discarded [32], [20]. They are cheap, lightweight, and high energy density, and are used primarily in portable electronic devices.

ii. Secondary batteries: This battery can store and transport electrical energy, which means that it can be charged and recharged multiple times. It can be charged by passing it in the opposite direction of the discharge current. [8]. They are more expensive than primary cells and are used in applications that involve some discharge and charge cycles, such as solar photovoltaic systems.

2.1.12. Specifying Batteries

When specifying suitable batteries for microgrid power management systems and standalone photovoltaic systems, the following factors need to be considered [9], [10].

i. Temperature correction: Most batteries are sensitive to extreme temperatures, and cold batteries cannot provide as much power as hot batteries.

ii. Depth of discharge: Compared to the total charge capacity, the percentage of the battery capacity (Ah) drawn from the battery is called the depth of discharge.

iii. Rated battery capacity: Represents the maximum energy the battery can produce in a single discharge under specified discharge rate and temperature conditions.

iv. State of charge (SOC): The state of charge is the remaining capacity of the battery at any time. It is equal to 1 minus the Depth of Discharge (DOD) given as a percentage.

v. Battery life cycles: The life span of any type of battery is difficult to determine, because it depends on many factors, such as depth of discharge, charge and discharge rate, operating temperature, and number of cycles.

vi. Days of autonomy: It refers to the number of days that the battery system continuously releases power under a given load without being charged by the photovoltaic system.

2.1.13. DC to DC Bidirectional Converter

A bidirectional converter is a device used to reduce or increase the voltage level, with the ability to flow power in the reverse or forward direction. The role of the bidirectional converter is to regulate the DC power flow from the bus voltage in both directions.

When the solar power generation system is used to generate electricity, the output will fluctuate, due to changes in environmental conditions. Due to the large fluctuations in production, the power system must always be connected to energy storage devices such as batteries. The battery stores excess energy during periods of low load demand and provides backup in the event of a system failure [11]. Therefore, a bidirectional converter is required to allow power to flow in both the forward and reverse directions.

2.1.14. Inverter

It is a device that converts direct current into alternating current [12]. As we all know, photovoltaic panels generate direct current and standalone photovoltaic systems have alternating current loads, so an inverter must be required to convert DC into AC power.

2.1.15. Charge Controllers

The charge controller is used to manage the current to and from the battery in the microgrid system. They are used to protect the battery and manage the DC bus voltage [13]. In a microgrid independent photovoltaic system, the charge controller will control the bidirectional converter by reducing the photovoltaic output voltage to reach the level required by the battery. When the photovoltaic output drops to zero, the charge controller will activate the bidirectional converter

The charge controller is usually a current and/or voltage regulator to prevent the battery from overcharging. It regulates the current and voltage from the photovoltaic panel and delivered to the battery. The main application of the charge controller is to provide the battery with the highest possible state of charge. In addition, it can also protect the battery from overcharging and disconnect the load to prevent over-discharge. If there is no charge control, regardless of whether the battery needs to be charged, the current from the photovoltaic module will flow to the battery in proportion to the irradiance [14]. If the battery is fully charged, improper charging will bring the risk of battery voltage rising to an extremely high level, resulting in internal heating of the battery, strong gas generation, accelerated network corrosion and electrolyte loss, so that the charge controller can provide health and increase battery life.

2.1.16. PID Controller

The PID controller is used to obtain better system dynamic constraints and reduce errors. For the work of this paper, the PID controller is combined with the fuzzy logic controller, which finds the error value and calculates the output value according to the error characteristic. There is a detailed description at the end of chapter three. The control variable will operate the bidirectional converter to control the energy flow between the battery and the microgrid to stabilize the autonomous photovoltaic voltage. PID controller contains three elements, such as P, I and D.

i. Proportional term: It makes a change to the output that is proportional to the current error value. It can be adjusted by multiplying the error by K_p which is known as proportional gain.

ii. Derivative term: The derivative of the process error is founded by determining the slope of the error over time and multiplying this rate of change by the derivative gain value [13], [15], [16].

iii. Integral term: Integral is proportional to both the magnitude of the error and the duration of the error.

2.1.17. Energy Management System

Energy management systems play a very important role in managing and sending loads from renewable energy sources to microgrid systems [17]. An efficient energy management system can not only save sustainable energy, but also minimize costs. The energy management system is essential for the stable operation of the microgrid, providing a high-quality power supply and flexible operation for loads and consumers [18].

The main objective of energy management is to improve the efficiency of the microgrid system and to use the energy given in the most prioritized way [19] and, [20]. In addition, the energy management system of the microgrid maintains the state of charge of the battery within a certain range, controls the charge and discharge of the battery, avoids over discharge/overcharge, and controls the frequent conversion of charge and discharge by the means of limiting the output power comes from the solar energy.

2.1.18. Energy Management Strategy

As we all know, solar power generation and load demand constantly change over time. Combining photovoltaic power sources to meet demand requires some reliability of the backup system and system switching between sources to adapt to changing needs. Therefore, the energy management strategy aims to meet the load demand and provide efficient solar energy. Therefore, in addition to photovoltaic energy sources, other energy sources such as batteries and power generation are also used. In addition, the DC voltage of the microgrid system remains unchanged [19] and, [18]. The EMS strategy can be used for autonomous systems with batteries.

The microgrid energy management standalone PV system flowchart is shown in Figure 2.9 and then, the process is described in three cases which are:

Case i: When the power generation (PG) and load demand (PL) are equal. In this case, the generated power by photovoltaic modules is equal to the total load of the ICT center, so the load will be supplied by the power generation without any disturbance. In the first case, the battery energy storage is not used, because there is no deficit or damped energy.

Case ii: When load demand is less than PV-generated power. In this condition, the excess power is transferred to the battery with consideration of the state of charge of the battery.

Case iii: When the load demand is greater than generated power from the PV modules. In this case, if the SOC of the battery is greater than the minimum value, the battery can meet the charging demand. In addition, if the battery SOC is lower than the minimum value, the system will not be able to meet the load demand, and there will be insufficient power. For energy storage, the SOC is between 30% and 85%.

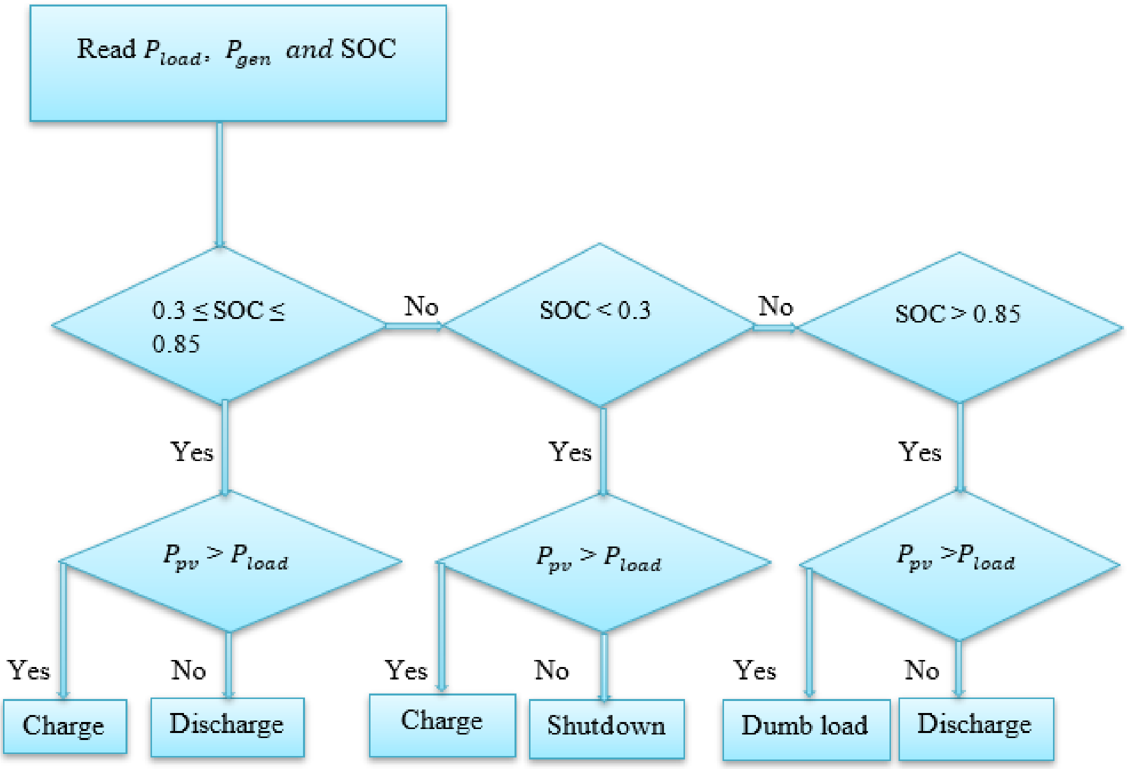

Figure 2.9. Flowchart of microgrid energy management system

2.1.19. Battery Management Systems

The Battery Management System (BMS) monitors the health of the battery by balancing the battery during charging or discharging, and uses key information by measuring current and voltage. BMS can estimate the state of charge of a battery using measured values and information such as battery life and the number of charge or discharge cycles [21]. BMS can also protect the battery from overcharge, undercharge, undervoltage, overvoltage and overcurrent.

2.1.20. Overall Microgrid Energy Management System and Control Standalone PV System

Generally, a microgrid is a power distribution system that includes distributed power, loads, energy storage devices, controllable loads, bidirectional converters, inverter, and control algorithms of the system is operated in a standalone or off-grid mode in this thesis work.

The power generation is connected to the DC bus, the AC electrical load is taken out of the DC power supply through the DC to AC converter, and then the AC power is supplied to the AC load through the inverter [22]. The microgrid power management system involves organizing power generation, charging, and storage of power or batteries to meet operational objectives such as cost, availability, and customer needs. Figure 2.10 below shows the entire microgrid power system.

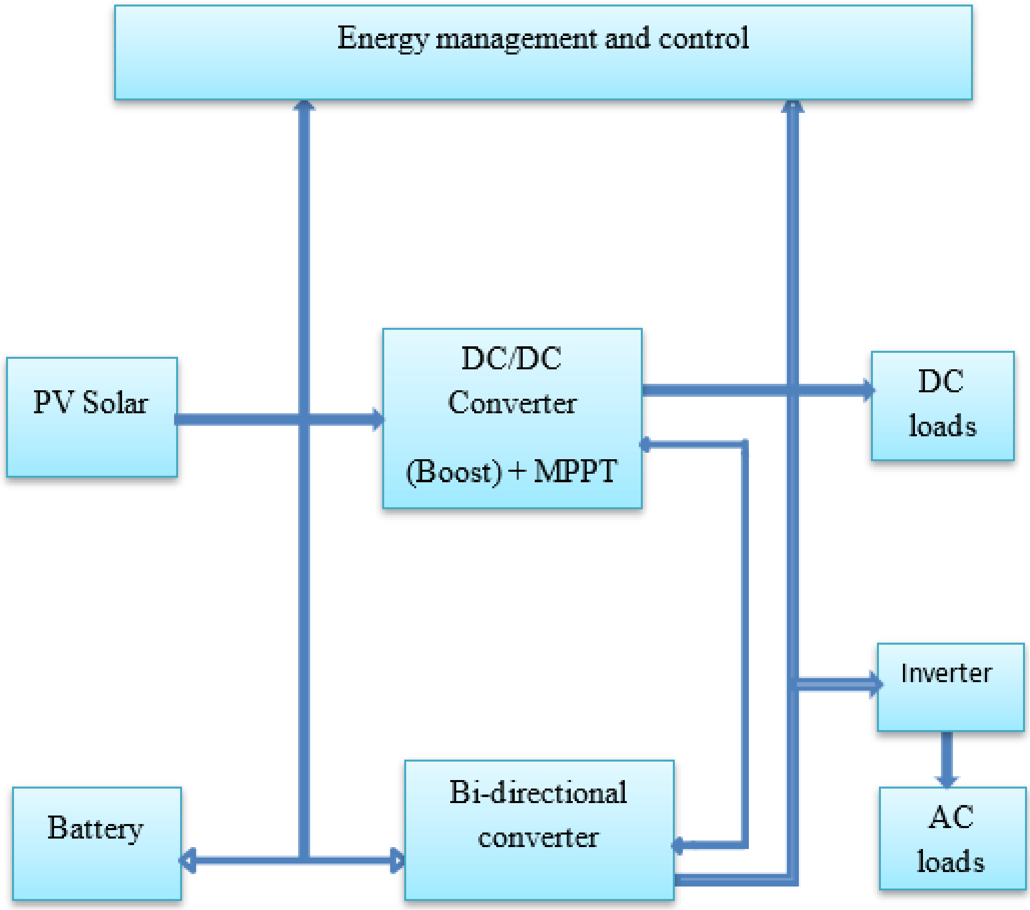

Figure 2.10. Block diagram of microgrid energy management of standalone PV system

In this paper, the EMS of the microgrid has a photovoltaic system powered by solar energy. It has a MPPT, which can extract the maximum power and improve efficiency through observation and perturbation methods. The DC-DC or boost converter controls the photovoltaic power according to its MPPT to increase the power generation of the microgrid system. Photovoltaic power directly supplied to DC power, and then converts the DC power to AC power through an inverter. In addition, the battery also stores energy and integrates with the photovoltaic array via a two-way converter. Also, to manage and control the microgrid energy management system, using fuzzy and fuzzy-PID controller are applied.

2.2. Related Work

Many researchers around the world have conducted research on the energy management and control system of the microgrid, especially some researchers in Ethiopia. Many authors have been studied based on renewable energy resources and the results have been published. Among them, some papers are reviewed in the next paragraph.

In [23], the modeling and simulation of DC microgrid. It was proposed that DC microgrid technology is based on renewable energy and system components such as photovoltaic panels, wind, maximum power point tracking, charge controllers and inverters. The author of this article takes the energy management and control of the DC microgrid system as an objective, and uses MATLAB / Simulink to establish a simulation model of the DC microgrid system, which is used for the electrification of small towns, and demonstrates the viability of the DC microgrid. Also, energy management control to improve the loading and unloading operations of the microgrid discussed. The DC microgrid uses a logic-based PI controller.

In [24], proposed the energy management of a DC microgrid with hybrid energy sources. The proposed work is to effectively and reliably manage the energy requirements of the system. The author's goal is to use a microgrid with unconventional energy sources such as solar energy to increase its productivity. In addition, the author uses diesel generators in the system. However, the use of diesel generators is not economical.

In [25], The modeling, design and analysis of independent photovoltaic DC microgrid systems are proposed. The proposed components of the system are solar photovoltaic systems, converters, incremental conductance, maximum power point tracking, bi-directional converters, batteries and DC to AC inverters. An intelligent control method using fuzzy logic control is proposed for MPPT control. The stability and analysis of DC microgrid system adopts step-up converter and bi-directional converter. It is recommended to use a standalone PV system with a DC microgrid to power both DC and AC loads. However, it is better to use fuzzy-PID controller rather than fuzzy-MPPT controller, in order to stabilize the system.

Also, according to in [26], the modeling, design and analysis of independent photovoltaic DC microgrid systems are discussed. The author's motivation is growing concern about global warming, rising natural gas prices, and oil energy pollution.

In [27], the control algorithm of the solar energy village micro-grid system is proposed. Based on the battery monitoring of the village solar microgrid system in Missouri, the author studied grid-connected mode and standalone mode. The solar village microgrid system design uses MATLAB/Simulink and the energy management algorithm is completed. In addition, the load control algorithm also plays a very important role in the system control algorithm. However, due to the lack of electricity in public services, the grid connection is very difficult to use.

According to in [28], the author studied the power management system controller of an isolated microgrid system located in a remote area of Papumpare in north eastern India to achieve power access. The author recommends using the system controller method developed in MATLAB/Simulink and integrating with HOMER PRO. The result obtained is to manage the energy flow from the power source to the load in a cost-effective and reliable way. The author did not include a bidirectional converter to stabilize the system.

In [29], a fuzzy logic control of a standalone system for photovoltaic energy conversion and renewable energy innovation is proposed. This study uses the maximum power point tracking function to maximize the power, adjust the charging power and control the battery operation. The improved fuzzy logic controller is used to adjust the battery operation method. The regulation of charging voltage is realized by PI controller. However, in order to further stabilize the system, a fuzzy-PID controller is better.

The author in [30], proposed a control and energy management strategy of standalone DC microgrid cluster using PV and battery storage for rural application. In this study, the operation of the DC microgrid and the behavior of the system at different operating conditions were evaluated under different conditions of the solar radiation and temperature changes for specific periods. The maximum power point trucking incremental conductance (MPPT-IC) algorithm was applied to maximize the efficiency and regulate the output voltage of the PV system to the desired DC bus voltage. The difficulty in this paper is the incremental conductance algorithm is reaching slowly the maximum power point for rapid change of irradiance. The system makes a lot of time to get the maximum power which leads to disturbance of power. To overcome this problem, using perturb and observe algorithm is reached first the maximum point rapidly than incremental conductance algorithm.

In [31], proposed the design, analysis and sizing of the PV/diesel/battery standalone hybrid power system using HOMER. The purpose of this proposed work is to simulate and optimize hybrid solar/diesel engine/residential energy storage. The components used in this article are photovoltaic solar energy, batteries, converters, diesel generators and inverters.

In addition, the author also demonstrated the use of HOMER software to reduce Total Net Present Cost (TNPC), Cost of Energy (COE), unsatisfied power load, and other cost parameters. The author demonstrated that the use of available solar energy resources can optimize dispatch and meet the energy demand curve. The difficulty of this work is that the use of diesel generators is costly and uneconomical. In addition, it will produce more smoke. Instead of using diesel generators, it is better to maximize the use of solar panels and choose the battery with the best capacity and efficiency.

In [32], a bidirectional DC to DC converter for solar battery backup applications is proposed. In this proposed work, a photovoltaic solar system with energy storage is realized with the help of a bidirectional converter. By using a PI controller, the output load is controlled. However fuzzy-PID is best controller than PI controller.

In [33], proposed the design of a standalone photovoltaic system for a typical household around Dessie city Ethiopia. The components used were PV array, charge controller, inverter, and battery storage. The size of the PV panel, inverter, battery, and cable is selected. Cost analysis of the system in US dollar's/kWh also calculated. But, the work of this author did not carry out the issue of modeling and no controller parts are applied.

In [34], proposed the design and optimization of the standalone photovoltaic system based on MPPT-FLC controller for electric bikes charging station. This author focuses on modeling, sizing, control, and simulation of PV off-grid system for Maadi region, Cairo, Egypt. The goal of the proposed PV system was to reduce the grid energy consumption and properly use renewable energy. HOMER software was applied for sizing and optimizing the PV system. Maximum power point tracking technique, based on the perturb and observe and fuzzy logic controller were applied for the controller. MATLAB/Simulink software was used for the modeling of the system. But compared with FLC and P and O controllers, Fuzzy-PID has better and faster response and steady-state output.

Generally, some papers are reviewed, which is related to this thesis work. Also, for each of papers reviewed, its limitations were tried to discussed. The drawbacks of this reviewed papers were: the use of diesel generators is not economical, bidirectional converter is not included, some modeling and controller parts are not applied, and the system are unstable, the incremental conductance algorithm is reaching slowly the maximum power point for rapid change of irradiance, which makes a lot of time to get the maximum power, and leads to disturbance of power. However, this thesis work is tried to solve the limitation of papers reviewed. The stable power system is provided, instead of using diesel generators, the solar panels and battery is selected which have best efficiency. Also, instead of using incremental conductance, the perturb and observe algorithm is selected, which is reached first at the maximum point rapidly than incremental conductance algorithm.

CHAPTER THREE

MATERIALS AND METHODS

3.1. Description of the Research Context

Currently, microgrids are used mainly in developing countries, especially Ethiopia, are used in industrial parks, universities and residential areas. The microgrid standalone PV-based system is recognized which is reliable and particularly important for the community. In this thesis work the study is to apply in Ambo University ICT center building which is in Ambo city and 110km far away from Addis Ababa, Ethiopia**.**

3.2. Research Method

The study was conducted by reviewing different kinds of literature related to the microgrid energy management system and control of the standalone photovoltaic system. In the work of this thesis, the microgrid obtains the generation of energy from photovoltaic systems and energy storage. The PV source is also classified into different components and the communities are getting enough electricity according to their demands. Appropriate equipment was selected by considering their demand with the best efficiency.

Microgrid energy management and control of standalone PV systems have been based on solar renewable energy resources. The modeling, analysis, optimization, and mathematically based microgrid have been done based on data collected from the selected area and others like NASA. Finally, the simulation results and conclusions are analyzed.

3.3. Methods of Data Collection

The data used in this thesis work were collected from the NASA and Ambo University ICT center building. Based on the demand, for ICT center building the required power has been estimated and appropriate materials were selected. Based on the collected data, the modeling and analysis of microgrid energy management and control of PV systems were done**.**

3.4. Methods of Data Analysis

Modeling and mathematical analysis are carried out by using different equipment for simulation in MATLAB. In addition, optimization is done by using HOMER PRO software to improve microgrid efficiency and minimize costs. Generally, the research of this paper includes modeling and analysis of the energy management system of the microgrid, and the control of the standalone photovoltaic system through the fuzzy-PID controller.

3.5. Solar Resource Data of Selected Site

Ambo is one of the Oromia region's cities in Ethiopia which is located 110 km from Addis Ababa; Ambo university ICT center building is found in Ambo city and found at latitude 7.67^0 N and longitude 36.83^0 that is taken from NASA. The following Table 3.1 shows Ambo University's ICT center building daily average solar insolation**.**

Table 3.1. Monthly averaged radiation (kWh/m^2/day)

Month	Jan	Feb	Mar	Apr	May	Jun	Jul	Aug	Sep	Oct	Nov	Dec
kWh/m^2/d	5.94	6.01	6.06	5.47	5.17	4.77	4.24	4.51	5.01	5.44	6.15	5.84

It can be seen from Table 3.1; the minimum radiation is 4.24kWh/m^2/day in July and the maximum average radiation is 6.15kWh/m^2 /day is gained in November. Ambo University areas are getting enough sun and it is suitable for microgrid standalone PV-based energy generation systems. The site location for the Ambo University ICT center building is found from NASA and it is shown in Figure 3.1 below.

Figure 3.1. Ambo University, western Shewa, Ethiopia, source (Google map)

3.6. Energy Demand and Load Estimation

Different kinds of loads are taken from the selected area in the ICT center building such as refrigerators, copiers, projectors TV sets, servers, network switches, and air conditioners. They are shown in the following Table 3.2.

Table 3.2. ICT center load demand and estimation

Loads	Quantity	Rating (W)	Adjusted Power (W)	Hrs./day	Energy/day (kWh/day)
Lighting	122	15	1830	8	14.64
Air-conditioner	8	1900	15200	2	30.4
Refrigerator	8	100	800	2	1.6
Printer	4	340	1360	1	1.36
Copier	4	300	1200	0.5	0.6
Desktop	140	80	11200	8	89.6
LCD Projector	2	280	560	2	1.12
Servers and cooling	2	500	1000	24	24
Network switches	4	370	1480	24	35.52
TV set	1	150	150	1	0.15
Total loads			Total watt = 34.78kW ≈35kW		Total energy = 198.99 ≈200kWh

Table 3.2 above describes all the appliances, their energy consumption and the number of operations. In addition, the total energy consumption of the electrical service of the ICT center building is described. The energy capacity of the total load is 200kWh.

3.7. Sizing of Standalone PV Systems and Procedures

The first step in starting to adjust the size of a standalone photovoltaic system is to determine the load consumption to be served. Therefore, the load estimation is based on the information taken from the ICT center building of Ambo University [35]. To determine the size of a standalone solar photovoltaic system, the first points to be estimated are:

- Building load estimation
- Sizing of the photovoltaic array and specification
- Sizing of the battery
- Sizing of the inverter
- Sizing of the battery charge controller
- Sizing of system cable
- Economic analysis

The following constant parameters are taken for sizing the photovoltaic system.

Table 3.3. Constant parameters used in photovoltaic array sizing [56].

No.	Description	Values
1	Battery efficiency	$0.8 < x < 0.85$
2	Temperature losses	0.9
3	Wire losses	0.9
4	Inverter efficiency	0.9
5	Depth of charge	0.85
6	Output efficiency	0.765
7	Combined efficiency	0.68

3.7.1. Sizing of the PV Array

Before sizing the PV array, the average energy demand in Watt-hour per day is obtained by estimating all appliances and the number of hours, they are used each day [36]. The steps to adjust the size are as follows:

Calculate total Watt-hours per day for each appliance used: Add the Watt-hours required for all appliances to get total watt-hours per day.

Calculate the total Watt-peak rating needed for PV modules: Divide the total watt-hours required by the combined efficiency and the PV modules per day by the average solar radiation to get the total maximum power [37]. Then the total peak power is divided by the DC voltage of the selected system to get the total PV current. Finally, the number of modules connected in parallel and in series can be determined by the following formula:

$$I_{pv} = \frac{\text{Peak power}}{\text{System DC voltage}} \tag{3.1}$$

$$N_s = \frac{\text{System DC voltage}}{\text{Module rated voltage}} \tag{3.2}$$

$$N_p = \frac{\text{Whole module current}}{\text{Rated current of one module}} \tag{3.3}$$

$$N_t = N_p \times N_s \tag{3.4}$$

where: I_{pv} is total PV current

N_s is number of series modules

N_p is number of parallel modules

N_t is total number of modules

3.7.2. PV Array Sizing

Load demand estimation of ICT center building (Ed) = 200kWh/day.

$$E_{pv} = \frac{\text{Energy demand}}{\text{Combined efficiencies}} \quad (3.5)$$

$$= \frac{200,000\text{Wh / day}}{0.68}$$

$$= 294,118\text{Wh/day}$$

The lowest average daily insolation is taken, (G min) = 4240Wh/m^2/d.

Step 1: PV array sizing

$$P_{pv} = \frac{E_{pv}}{G_{min}} \times 1000\text{W / m}^2 \quad (3.6)$$

where: P_{pv} is the total power of PV array in watts

E_{pv} is the total energy required from the PV array

G_{min} is the minimum solar radiation of a month that occurred in a year.

Therefore, using Equation (3.6)

$$P_{pv} = \frac{294,118}{4240} \times 1000 = 69368\text{W}$$

Step 2: By using Equation 3.1, total PV current is calculated as follows:

$$I_{pv} = \frac{69368\text{W}}{400} = 174\text{A}$$

Therefore, the PV module for design purposes (CSS-MSP-250W is selected.

Step 3: Number of PV modules in Parallel is found using Equation (3.3).

$$N_p = \frac{174\text{A}}{7.79\text{A}} = 22.33 \approx 25 \text{ modules}$$

Step 4: Number of series modules is found using Equation (3.2)

$$N_s = \frac{400}{30.8} = 12.98 \approx 13 \text{ modules}$$

Step 5: Total number of modules using Equation (3.4): $N_t = N_p \times N_s = 25 \times 13 = 325$ modules

3.7.3. Total Area of Solar Panels Design

In the photovoltaic system design process, the size of the area covered by the solar module is very necessary, therefore, considering the length and width of the photovoltaic module:

L = 1640mm, W = 990mm

Area of single module is A = L × W (3.7)

Total area of solar panel is = $(L \times N_p) \times (W \times N_s)$ (3.8)

A = (1640mm × 25) × (990mm × 13)

A = 527,670,000mm^2 = 528m^2

3.7.4. Battery Sizing

Step 1: Energy consumption of battery:

$$E_b = \frac{\text{Energy demand} \times \text{days of autonomy}}{\text{Efficiency} \times \text{DOD} \times \text{nominal battery voltage}} \quad (3.9)$$

where: Energy demand (E_d) = 200kWh/day

Days of autonomy (N) = 2

Depth of discharge = 0.85

$$E_b = \frac{(200,000 \text{ x } 2)}{0.85 \times 0.765} = 615,148.02\text{Wh/day}$$

Step 2: Battery Ampere hour capacity:

$$C_{bat} = \frac{E_b}{V_{nominal}} = \frac{615,148.02}{400} = 1538\text{Ah}$$

Select the battery, which is any kind, 12V nominal and 200Ah rating from the specification of deep cycle battery.

Step 3: Battery required for parallel:

$$B_{parralel} = \frac{C_{bat}}{Ah_{\text{rating of battery}}} \quad (3.10)$$

$$B_{parralel} = \frac{1538}{200} = 7.69 \approx 8$$

Step 4: Battery required for Series (B_{series}) = $\frac{V_{system}}{V_{bnominal}} = \frac{400}{12} = 33.33 \approx 34$

Step 5: The total number of batteries required = $B_{series} \times B_{parallel}$ = 8×34 = 272 batteries

3.7.5. Charge Controller Sizing

The size of the charge controller depends on the maximum charge current of the photovoltaic array and the rated current of the charge controller. [38].

$$\text{Current controller rating} = 1.25 \times I_{sc} \times N_p \quad (3.11)$$

where: 1.25 is the safety factor for sizing PV systems

I_{sc} is the short circuit current of the PV module

N_p is the number of solar modules connected in parallel.

Therefore, the current controller rating = 1.25 × 8.49 × 25 = 265.31A

Therefore, based on values of current controller rating, 12V, 60Ah MPPT based solar charge controller have been chosen from specifications.

$$\text{Number of charge controllers} = \frac{\text{Total current controller rating}}{\text{Controller rating from specification}} \quad (3.12)$$

$$= \frac{265.31\text{A}}{60\text{A}} = 4.4 \approx 5$$

3.7.6. Inverter Sizing

To determine the size of the inverter, it must be able to handle the expected maximum power of the AC load. Therefore, 25-30% greater than the total AC rated power should be considered [33]. The rated power of the inverter becomes 32950 + (0.26 × 32950) = 41517 W, so the selected inverter is CSI-10KTL1P-GI-FL, and the inverter is 11.5 KW × 4, which can operate at the continuous nominal power required by the photovoltaic system.

3.7.7. Cable Sizing

Low voltage batteries, solar panels, cables and loads require particular wire sizes. It must be the correct size, otherwise if it is too small it can be dangerous and cause heating, fires and wasted energy. The following steps are followed to determine the cable size [39].

Table 3.4. Values of parameters used for cable sizing [60].

Description	Value
Length of cable	12m
Conductivity of copper	58×10^{-6} s/m
Resistivity of copper	$1.72 \times 10^{-8}\ \Omega$

The maximum current of the charge controller is defined as 125% times the rated short-circuit current (I_{sc}) from PV specification.

$$I_{max} = 1.25 \times 8.49 \times 25 = 265.31A$$

Generally, the cross-sectional area of the cable is given by the following formula [59].

$$A = \frac{2 \times l \times I}{Conductivity \times V_d} \tag{3.13}$$

where: ρ is the resistivity of copper wire

A is the cross-sectional area

V_d is the maximum allowable voltage drops

l is the length of the cable and

I is the maximum current that can be carried by the cable or the conductor.

$$A = \frac{2 \times 10 \times 265.31}{58 x 10^6 \frac{s}{m} \text{ x } 0.03 \times 400} = 8.66mm^2$$

Therefore, $10mm^2$ is chosen from cable standard.

The maximum charge controller to load current = $\frac{\text{Total load power}}{\text{System voltage}} = \frac{35000W}{400V} = 87.5A$

To calculate the cable size between load and charge controller, the given voltage losses are 5%, length 10m, and 90A.

$$A = \frac{2 \times 10 \times 90}{5 \times 10x^6 \times 0.05 \times 400} = 1.55mm^2$$

Thus, the chosen area is $2.5mm^2$ from cable standard.

The cross-sectional area of cable, between the charge controller and battery, the voltage losses, is 0.02, length 10m and 160A.

$$A = \frac{2 \times L \times I}{58 \times 10^6 \times V_{drop} \times 400} \tag{3.14}$$

$$A = \frac{2 \times 10 \times 160}{58 \times 10^6 \times 0.02 \times 400}$$

$$= 3.88mm^2 \approx 4mm^2$$

To determine the cable size between load and inverter, it assumed that the length of the cable for powering the load from the inverter is 10m and the voltage drop is 0.04 [39]. So, the maximum current is given by:

In the case of a three-phase inverter, the maximum current given by:

$$I_{max} = \frac{I_{inverter\ KVA}}{\sqrt{3} \times V_{out}} \quad (3.15)$$

In the case of a single-phase inverter, the maximum current given by:

$$I_{max} = \frac{I_{inverter\ KVA}}{V_{out}} \quad (3.16)$$

Therefore, the cable cross-sectional area between the load and the inverter is calculated as follows: $A = \frac{2 \times 15 \times 50}{58 \times 10^6 \times 400 \times 0.04} = 1.06mm^2$.

So, from cable standard the chosen cable is $1.5mm^2$.

3.7.8. Economic Analysis

The net present cost, and cost of energy are the most important evaluation tool for the economic behavior of renewable energy systems. It provides all system component's costs, capital cost, replacement cost, operation, and maintenance cost. The initial capital cost of the system is the cost required to purchase all the components of the system, such as photovoltaic panels, batteries, charge controllers, converters, inverters, and installation (including wiring, etc.).

Operation and maintenance costs are also annual recurring expenses for system management, construction management, and regular maintenance. To continue to function and provide efficient system performance, certain system components must be replaced regularly in accordance with their type and operating conditions. [35], [40]. Cost estimation of the microgrid standalone PV system is discussed as following with specifications.

- The capital cost of the system (initial cost) is high.
- Maintenance costs are very low.
- There are no fuel costs.
- Replacement costs are low.

$$\text{Replacement cost} = A_1 \left(\frac{1+i}{1+d}\right)^n \quad (3.17)$$

where: A_1 is the initial cost of the battery, inverter, charge controller, and converter.

n is a lifetime in years

i is a inflation rate of 4%

d is a discount rate of 8%

Table 3.5. Cost of microgrid component [41], [42]

No.	Component	Capital cost ($)	Replacement cost ($)	O&M cost($/year)	Lifetime (years)
1	PV panel	162,500$	76392$	3130$	20
2	Converter	3907$	2679$	100$	10
3	Battery	21760$	25150$	420$	10
4	Inverter	21392$	10057$	100$	20
5	Charge controller	1475$	1011.32$	-	10

where the PV panel initial cost is 2$/W × 325 × 250W = 162,500$

Inverter cost is 21392$, and charge controller is 295$ × 5 = 1475$, and for battery is 80$ × 272 = 21760$

Using Equation (3.17) the following replacement costs are calculated as:

Replacement cost of PV panel = $=162500\$\left(\frac{1+0.04}{1+0.08}\right)^{20}$ = 76392$

Replacement cost of converter $=3907\left(\frac{1+0.04}{1+0.08}\right)^{10}$ = 2679$

Replacement cost of inverter $=21392\left(\frac{1+0.04}{1+0.08}\right)^{20}$ = 10057$

Replacement cost of charge controller $=1475\left(\frac{1+0.04}{1+0.08}\right)^{10}$ = 1011.32$

The annual operation and maintenance costs of photovoltaic panels can be calculated based on the initial capital cost, considering the discount rate and the inflation rate as follows:

$$O\ \&\ M = 2\%PV \times \frac{1+i}{1+d} \times \left[\frac{1 - (\frac{1+i}{1+d})}{1 - (\frac{1+i}{1+d})} \right]^{n} \tag{3.18}$$

$$O\ and\ M = 0.02 \times 162500\$ \times \frac{1+0.04}{1+0.08} \times \left[\frac{1 - (\frac{1+0.04}{1+0.08})}{1 - (\frac{1+0.04}{1+0.08})} \right]^{20} = 3130\$$$

The battery's operation and maintenance are calculated as O and M cost of PV panel. Battery life is estimated at 10 years, so it should be replaced twice during the life of the system [40]. The cost of battery replacement is calculated for the first time after 10 years, and the cost for the second replacement after 20 years is calculated as follows.

$$B_{rep1} = B_c \left(\frac{1+i}{1+d} \right)^{n} \tag{3.19}$$

$$B_{rep1} = 21760\$ \times \left(\frac{1+0.04}{1+0.08} \right)^{10} = 14920\$$$

$$B_{rep2} = 21760\$ \times \left(\frac{1+0.04}{1+0.08} \right)^{20} = 10230\$$$

Battery replacement cost = B_{rep1} + B_{rep2} = 14920$ + 10230$ = 25150$

where: B_{rep1} and B_{rep2} are replacement times after 10 and 20 years respectively [40].

Using from above Table 3.5, the total replacement cost, O and M cost were calculated as following: The total replacement cost is the total replacement cost of converter, charge controller, inverter, battery, PV panel and calculated as follows:

Total replacement cost = 76392$ + 2679$ + 25150$ + 10057$ + 1011.32$ = 115289.32$

Th total O and M cost is the total cost of O and M of PV panel, Battery, Inverter, and Converter. Total O and M cost = 3130$ + 420$ +100$ + 100$ = 3750$

For installation cost 10% of PV panel initial cost is taken which is = 0.1× 162500$ = 16250$

The net present cost of the microgrid system is calculated by adding all the costs of PV components, batteries, total replacement costs, controller inverters, installation, operation and maintenance costs.

Net present cost = $PV_c + C_c + B_c + Inv_c + Ch_c + Inst_c + \text{Total rep}_c + O\&M$ (3.20)

Using Equation (3.20) the NPC is calculated as:

NPC = 162,500$ + 3907$ + 21760$ + 21392$ + 1475$ + 16250$ + 115289.32$+ 3750$

= 346,323.32$

where: PV_c is capital cost of photovoltaic panel, C_c is converter cost, B_c is battery cost, Ch_c is charge controller cost, and $Inst_c$ is installation cost.

In addition, it is also important to calculate the total annual cost of the system $/year. The total annualized cost $/year of the microgrid system in terms of the currently the dollars can be evaluated using the following Equation (3.21). Total annualized cost [$/year] can be calculated as the following [40], [43].

Total annualized cost [$/year];

$$C_{ann,tot} = NPC \times \left[\frac{i \times (i+1)^n}{(1+i)^n - 1} \right] \quad (3.21)$$

$$CRF = \left[\frac{i \times (i+1)^n}{(1+i)^n - 1} \right]$$

where: CRF is the capital recovery factor.

Using Equation (3.21), the total annualized cost calculated as:

$$CRF = \left[\frac{0.04 \times (0.04+1)^{20}}{(1+0.04)^{20} - 1} \right] = 0.073582$$

$$C_{ann,tot} = 346{,}323.32\$ \times 0.073582 = 25{,}484\$$$

Levelized cost of energy: The HOMER PRO software defines the levelized cost of energy as the average cost/kWh of useful electricity generated by the microgrid system [35]. The cost of energy can be found from the total annual cost and the annual energy produced by the photovoltaic system and shown in Equation (3.22).

$$COE = \frac{C_{ann,tot}}{365 \times E_{load}} \quad (3.22)$$

$$\text{COE} = \frac{25,484\$}{365 \times 200\text{kwh / yr}} = 0.349\$/\text{kWh}$$

Here, the cost of the proposed for this standalone microgrid energy system is higher than the cost set by the Ethiopian electric utility company. However, this may be an acceptable alternative, because of its efficiency, reliability, and other areas where power is not available.

3.8. Modeling of Microgrid Energy Management Control Standalone PV System

3.8.1 Photovoltaic Model

Photovoltaic modules include many photovoltaic cells connected in series and in parallel to provide high output voltage and increase photovoltaic current respectively. The direct current of photovoltaic energy generated by the photovoltaic array depends on temperature and solar irradiance [44], [45], and [46]. The PV model with a single diode circuit, series resistance, and parallel are the most commonly used in PV modeling and to predict energy production in photovoltaic cells.

The following PV model used a different method to calculate the parameter of the system [47]. The parameters of the selected PV array (CSS-MSP-250W) are given in Table 3.4 which is important to model the PV array.

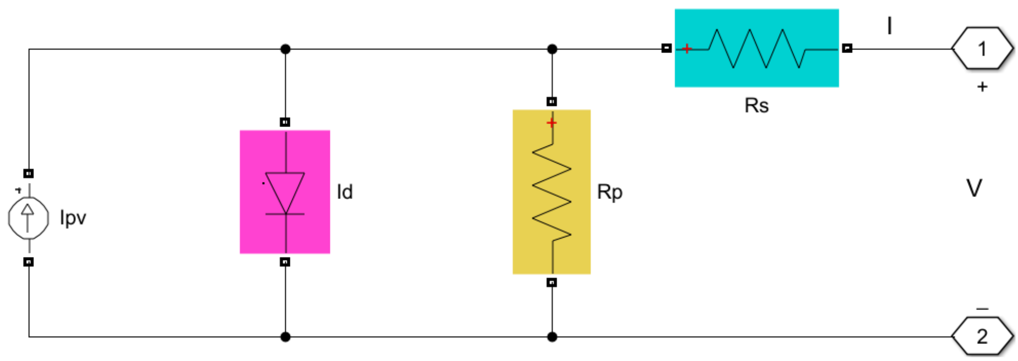

Figure 3.2. Equivalent circuit of PV model using single diode along with series and parallel resistances [43].

The mathematical model of a PV cell can be described in the following equations [46], [44]. From an equivalent circuit diagram Figure, 3.2 using Kirchhoff's current law is applied.

$$I = I_{pv} - I_d - \frac{V_d}{R_p} \tag{3.23}$$

$$I_d = I_o \; [\exp (q \, (\frac{V_{pv} + I_{pv} R_s}{a \times K \times T}) - 1] \qquad (3.24)$$

$$I_p = (\frac{V_{pv} + I_{pv} R_s}{R_p} \qquad (3.25)$$

By applying Equations (3.24), (3.25) into (3.23) the equivalent circuit is found.

$$I = I_{pv} - I_o \, [\exp (q \, (\frac{V_{pv} + I_{pv} R_s}{a \times K \times T}) - 1] - (\frac{V_{pv} + I_{pv} R_s}{R_p}) \qquad (3.26)$$

From Equation (3.26), also light generated current I_{pv} and I_o are found as:

$$I_{pv} = \frac{G}{G_n} (I_{pvn} + K_i \left(T - T_{ref} \right) \qquad (3.27)$$

$$I_o = \frac{I_{sc} + K_i \Delta T}{\left(\exp \frac{V_{oc} + K_v \Delta T}{V_t \times a} \right) - 1} \qquad (3.28)$$

PV module model consists of modules connected in series (N_s) and parallel (N_p).

Therefore, Equation (3.26) is replaced by the following Equation (3.29):

$$I = ((N_p I_{pv} - N_p I_o) \, [\exp [(V + IR_s \times (N_s) / \left(N_p \right)) / \left(a V_t N_s \right)] - 1])) \qquad (3.29)$$

where: R_s is the series resistance (Ω)

R_p is the shunt resistance (Ω)

a is the diode ideality factor

K is the Boltzmann constant (1.38×10^{-23}) JK^{-1}

q is the electronic charge (1.602×10^{-19})

N_s is the number of cells connected in series

N_p is the number of cells connected in parallel

I_{scn} is the short-circuit current at the nominal condition

T is module operating temperature in Kelvin

I_{pv} is the light generated current of the photovoltaic cell

I_d is the diode saturation current

V_d is the voltage across the diode

G is the actual irradiance in W/m^2

G_n is the irradiance at the nominal condition

V_{ocn} is the open circuit voltage at the nominal condition

V_{tn} is the voltage thermal at the nominal condition

ΔT is deviation from the nominal temperature in Kelvin.

Table 3.6. Electrical characteristics for photovoltaic array specification [66].

Description	Value
Peak Power (P_{max})	250W
The voltage at P_{max} (V_{mp})	30.8V
Current at P_{max} (I_{mp})	7.79A
Open-circuit voltage (V_{oc})	37.4V
Short-circuit current (I_{sc})	8.49A
Power tolerance	±3%
Series fuse rating (A)	15
Parallel resistance of PV model (ohms)	43.15
Series resistance of PV model (ohms)	0.847
Cell efficiency	17.24%
Current temperature coefficient $\alpha\,(I_{sc})$	0.03%/ ^{0}C
Voltage temperature coefficient β (V_{oc})	- 0.32%/ ^{0}C
Power temperature coefficient γ (P_{max})	-0.42%/ ^{0}C

The parameter of the PV model mathematical equation is calculating as the following [48], [49].

$$R_s = \frac{V_{oc} - V_{mp}}{I_{mp}} \tag{3.30}$$

$$R_p = \frac{I_{sc} R_s - V_{oc}}{I_{mp} - I_{sc}} \tag{3.31}$$

$$I_{ph} = \frac{I_{sc} \times \left(R_s + R_p\right)}{R_p} \tag{3.32}$$

$$R_s = \frac{37.4 - 30.8}{7.79} = 0.847\ \Omega$$

$$R_p = \frac{(8.49 \times .847) - 37.4}{7.79 - 8.49} = 43.15\ \Omega$$

A PV array is modeled based on the mathematical Equation of the solar system using MATLAB/Simulink blocks. The necessary parameters used in PV array modeling such as V_{oc}, I_{sc}, N_s, N_p, K_t, T_{ref}, and G are taken from the specification of the PV array.

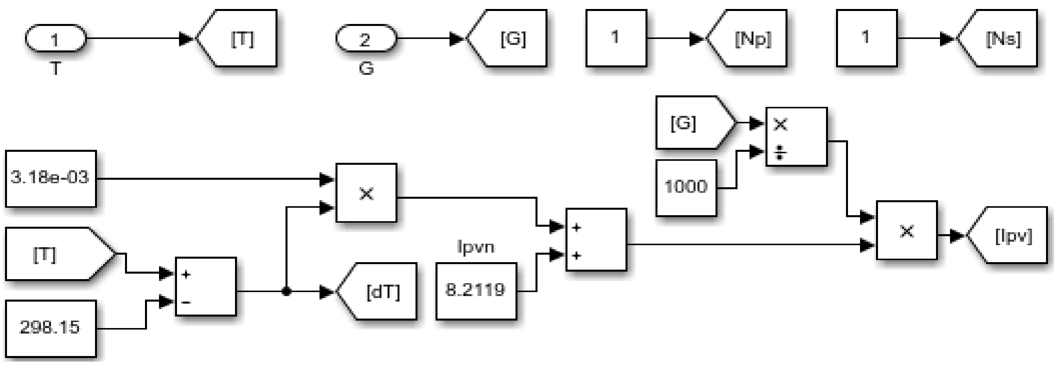

Figure 3.3. Subsystem simulink of light generated current

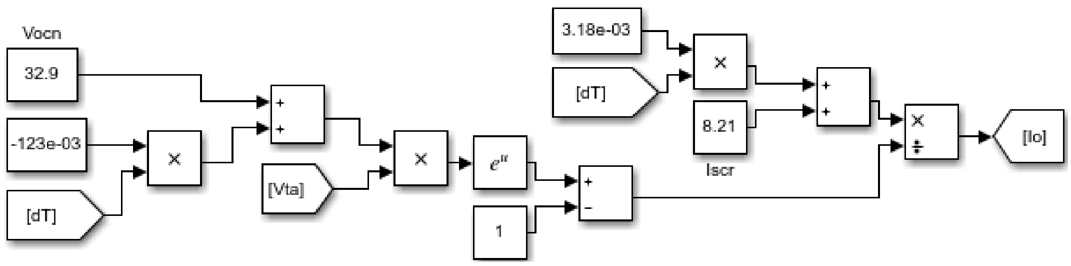

Figure 3.4. Subsystem simulink of saturation current

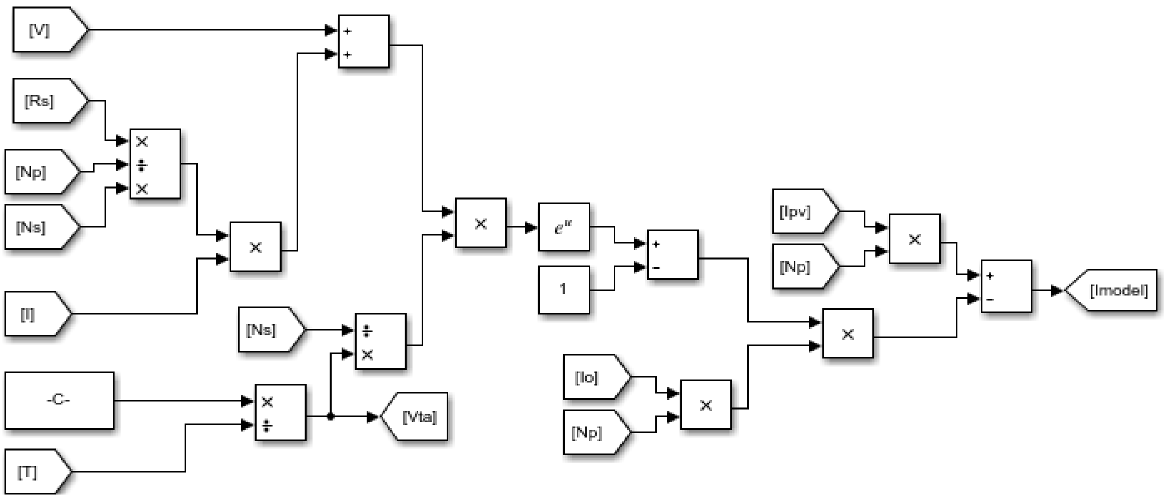

Figure 3.5. Subsystem of simulink diagram of the photovoltaic current

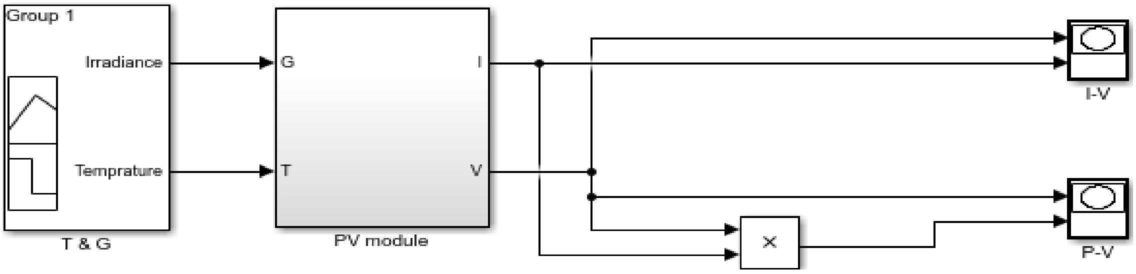

Figure 3.6. The Simulink diagram of photovoltaic module

Under various temperatures and irradiances, the relationship between the current and power of photovoltaic modules can be found. The fixed temperature is 25°C with the change of irradiance, the characteristic curves I-V and P-V are drawn with G = 400W/m^2, 600W/m^2, 800W/m^2 and 1000W/m^2, respectively. The curve is not linear and depends on temperature and solar radiation. As the irradiance increases, the current increases more than the voltage, and the maximum power point also increases, as shown in Figure 3.7.

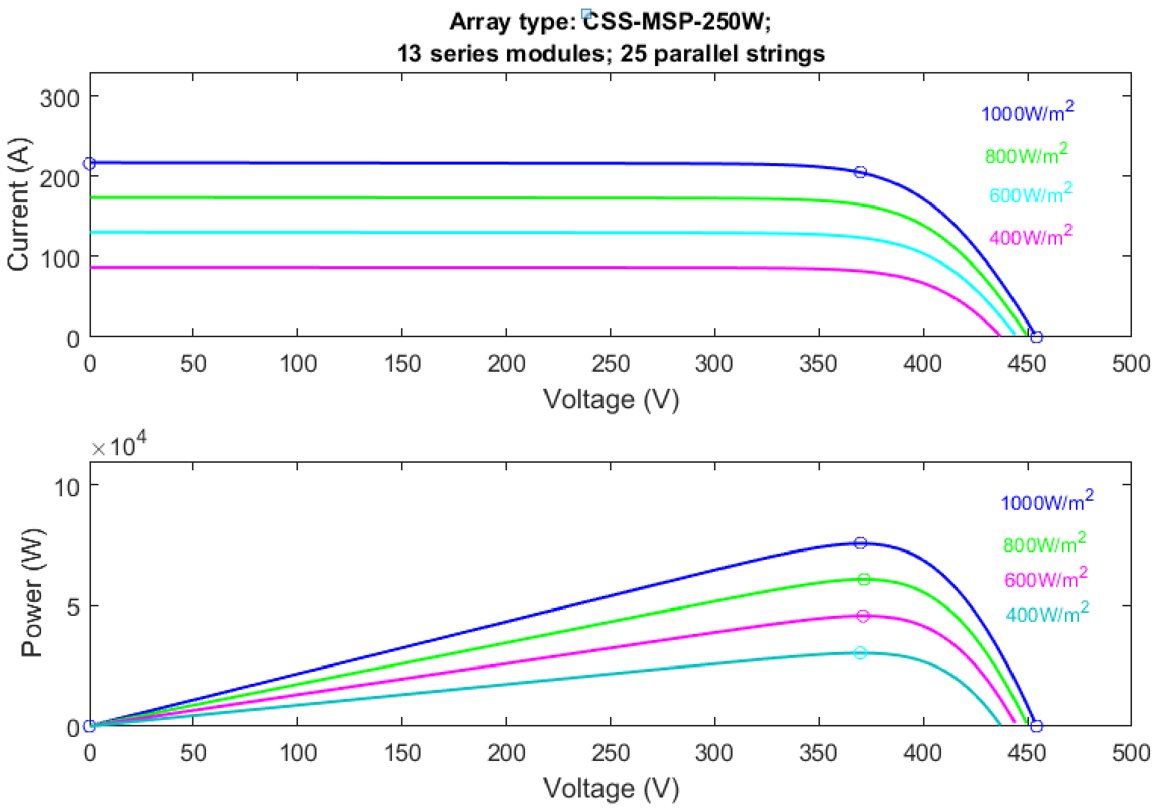

Figure 3.7. V-I and P-V characteristic with variable solar radiation

Figure 3.7 above describes the maximum output power of the photovoltaic array that increases with increasing irradiance at a fixed temperature. The response of the photovoltaic array to different values of solar radiation and a fixed temperature has a significant impact on the short-circuit current. However, the impact on the open circuit voltage is minimal. Therefore, when solar radiation increases, the photovoltaic array produces more energy.

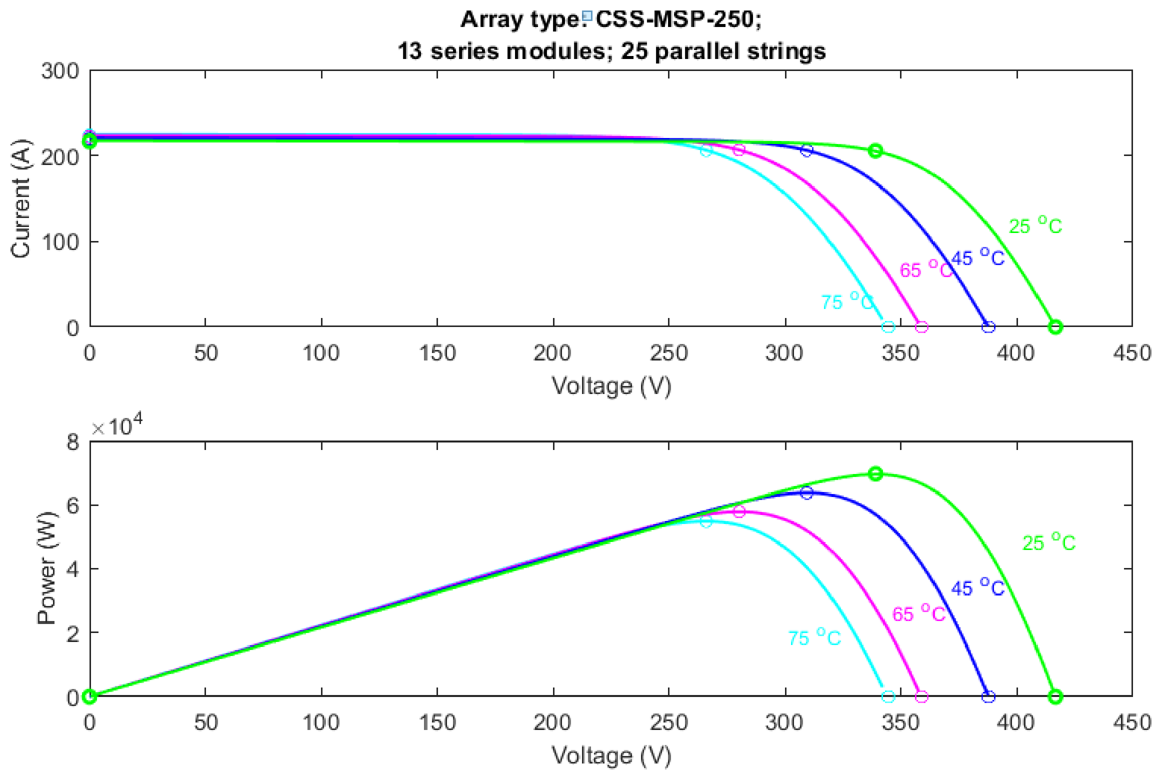

Figure 3.8. I-V and P-V characteristic with constant solar radiation

Figure 3.8 above shows that temperature has a significant effect on open circuit voltage and has no effect on power and current. However, when the temperature drops, the photovoltaic array produces more energy.

3.8.2. Modeling of Boost Converter

There are three main types of DC to DC converters: Boost converter, buck converter, and buck-boost converter [50], and [44]. The mathematical equations for the parameter of boost, buck, and buck-boost converter were determined using the following Equations:

$$V_{out} = \frac{V_s}{1 - D} \quad \text{or } D = 1 - \frac{V_{in}}{V_{dc}} \tag{3.33}$$

$$V_{out} = D\,V_s \tag{3.34}$$

$$V_{out} = -Vs\left(\frac{D}{1-D}\right) \qquad (3.35)$$

$$L_{min} = \frac{(1-D)\times D\times R}{2f_s} \qquad (3.36)$$

$$C_{min} = \frac{D\times V_{out}}{R\times f_s\times V_r} \qquad (3.37)$$

$$\text{where: } V_r = \frac{\Delta V_{out}}{V_{out}}, \text{ and } R = \frac{Vout^2}{P_{in}}$$

In this thesis, the reference DC link voltage is 400V, the DC link voltage ripple is taken as 1% of DC link voltage, so 1% of 400V is 4V and the switching frequency is 10 kHz and 5% deviation from the nominal output voltage to get the duty cycle [49]. The boost converter circuit is shown in Figure 3.9. Main parameters such as inductance, capacitance, diode and resistance are designed. Diodes are used to protect the photovoltaic array from negative currents. The capacitor is placed here to limit high frequency harmonics.

$$V_r = \frac{376V}{400} = 0.94V$$

$$L_{min} = \frac{(1-0.05)\times 0.05\times 1.89}{2\times 10000} = 4.5\mu H$$

$$C_{min} = \frac{400\times 0.05}{1.89\times 10000\times 0.94} = 1.12mF$$

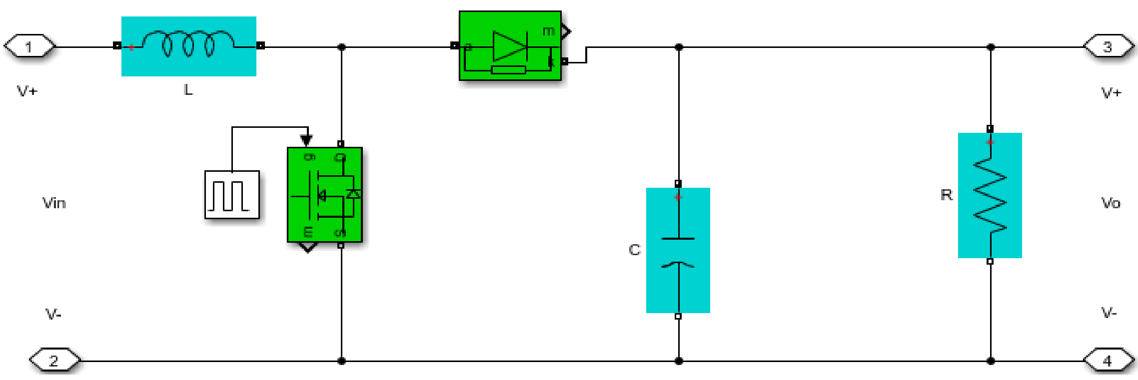

Figure 3.9. Modeling of the boost converter

3.8.3. DC to AC Converter (Inverters) Modeling

The DC-AC converter is used to convert the DC output voltage of the photovoltaic array into AC voltage. It consists of a resistor and four power switch blocks. Pulse width modulation (PWM) is used for inverter modeling to obtain a suitable switching trigger signal to control the amplitude and frequency of the output voltage. Capacitors are used to filter noise on the DC bus link.

In the work of this thesis, a single-phase inverter is used. This is DC to AC, which converts the DC power from the PV into AC power at the desired output voltage and frequency. The power supply designed in this research is to convert the output voltage from 400V DC to 220-250V AC at a frequency of 50 Hz. Figure 3.10 shows a typical IGBT-based DC to AC inverter configuration. IGBT2 and IGBT4 allow current to flow in one way, while IGBT2 and IGBT3 allow current to flow in the opposite polarity.

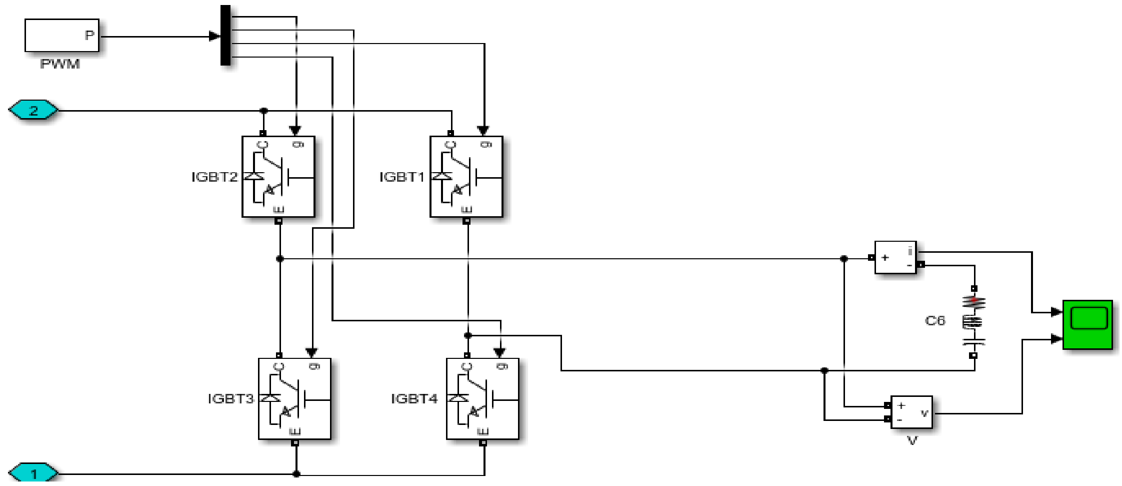

Figure 3.10. DC-AC converter (inverter) modeling

3.8.4. Battery Modeling

Due to the fluctuating characteristics of the photovoltaic array, the battery is the basic element of the independent microgrid photovoltaic system [51]. A simple modeling equivalent circuit of a rechargeable battery is shown in Figure 3.11.

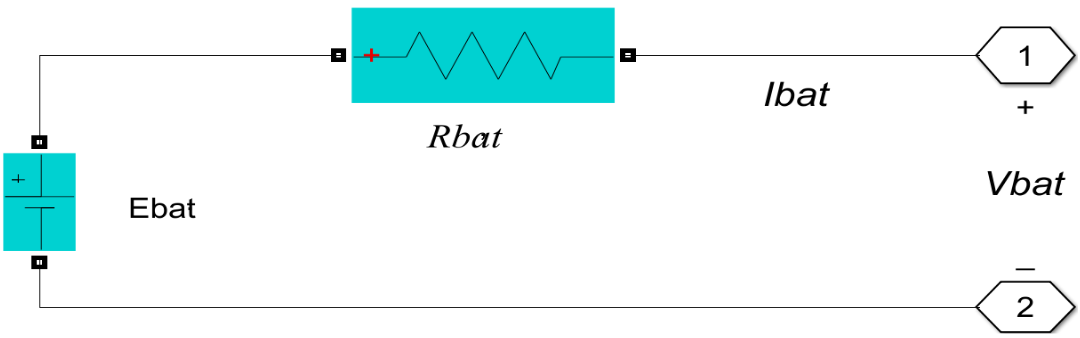

Figure 3.11. Simple equivalent circuit of rechargeable battery modeling [51].

Applying the KVL law, the voltage in battery storage can be obtained as follows [52].

$$V_{bat} = E_{bat} - R_{bat} I_{bat} \tag{3.38}$$

$$P_{bat} = V_{bat} I_{bat} \tag{3.39}$$

It is necessary to use a control energy storage to provide its lifespan. So, the state of charge is a basic parameter used in battery charging and discharging. SOC is the criterion for determining the charging or discharging of the battery, and it is shown in Equation 3.39.

$$SOC = \frac{Q_c}{Q_r} \times 100\% \tag{3.40}$$

where: P_{bat} is battery power delivered to the load

R_{bat} is the internal resistance of the battery bank

I_{bat} is battery current to the load

Q_c is remain capacity of the battery (Ah)

Q_r is rated capacity of the battery (Ah)

The battery or energy storage is modeled as a non-linear voltage source, the output voltage of which depends on the state of charge, and the current, voltage and internal resistance also depend on the state of charge [13].

3.8.5. Bidirectional DC to DC Converter Modeling

A system includes a battery with a bidirectional DC-DC converter that is used to interconnect battery power to the DC system [53], and [54]. The main function of the bidirectional DC-DC converter is to control the power and voltage requirements of the DC link and to control the amount and direction of the power supplied to/from the battery.

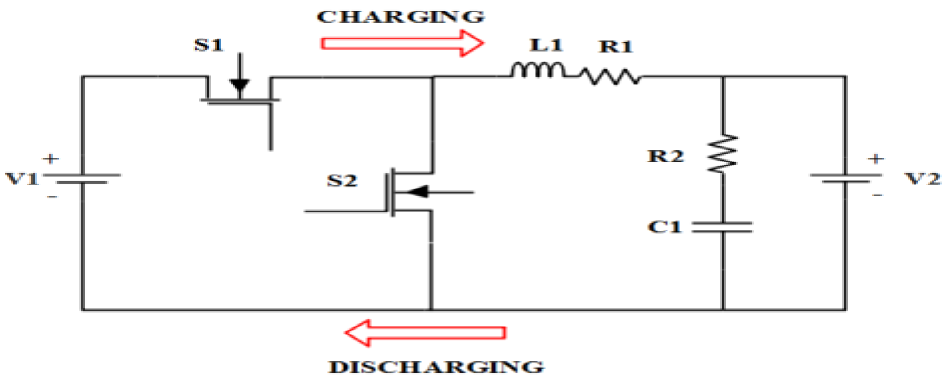

Figure 3.12. Circuit diagram of the bidirectional DC to DC converter [54].

The bidirectional DC-DC converter should convert photovoltaic energy into stable and reliable electrical energy required for battery charging. In the case of the "buck" mode, the bidirectional DC-DC converter is used to reduce the output voltage of the system. [54]. The bidirectional DC-DC converter has two modes of operation:

Mode i: When the DC link voltage is higher than the reference value, the bidirectional DC-DC converter operates in buck mode. In this operating mode, the converter controls the current to charge the battery.

Mode ii: When the DC link voltage is lower than the reference value, the bidirectional DC-DC converter operates in boost mode. In this mode, the photovoltaic system sends its energy to the battery and vice versa. The bidirectional DC to DC converter (buck-boost) consists of two main switches (S1, S2) with a capacitor and an inductor. The switch is responsible for managing the buck and boost modes. The duty cycle of the bidirectional buck-boost converter can be obtained by the following formula (3.41).

$$D = \frac{V_o}{V_o + V_{in}} \tag{3.41}$$

$$= \frac{400}{400 + 369.8} = 0.51$$

The output current of the converter is $I_{out} = \frac{I_{in}}{D_1}(1 - D_2)$ (3.42)

$$= \frac{86}{0.51}(1 - 0.51) = 82.6A$$

where $D = D_1 = D_2$

Taking into account the worst-case safety of the converter, the current ripple rate is 200%. The critical value of inductance (L) becomes:

$$L_c = \frac{V_{in} T}{K_i I_{in}} \times D \tag{3.43}$$

Using Equation (3.42), $L_c = \frac{369.8\left(\frac{1}{10000}\right)}{200 \times 86} \times 0.51 = 1.14\mu H$

$$L = 1.5 \times L_c = 1.71\mu H$$

$$C_1 = \frac{D_2}{K f R} \tag{3.44}$$

$$C_1 = \frac{0.51}{0.05 \times 10000 \times 0.35} = 29mF$$

Furthermore, the transfer function of the bidirectional converter is shown in the following equation (3.45).

$$\frac{V_o(s)}{V_{in}(s)} = (D-1)\left[\frac{\frac{1}{LC}}{S^2 + \frac{1}{RC} S + \frac{(1-D)^2}{LC}}\right] \tag{3.45}$$

Note that during charging and discharging, the output voltage ripple is set to 5%. The DC voltage system is controlled by managing the duty cycle through the bi-directional converter [55], [56]. It also keeps up as a steady voltage at the required side for both buck and boost modes.

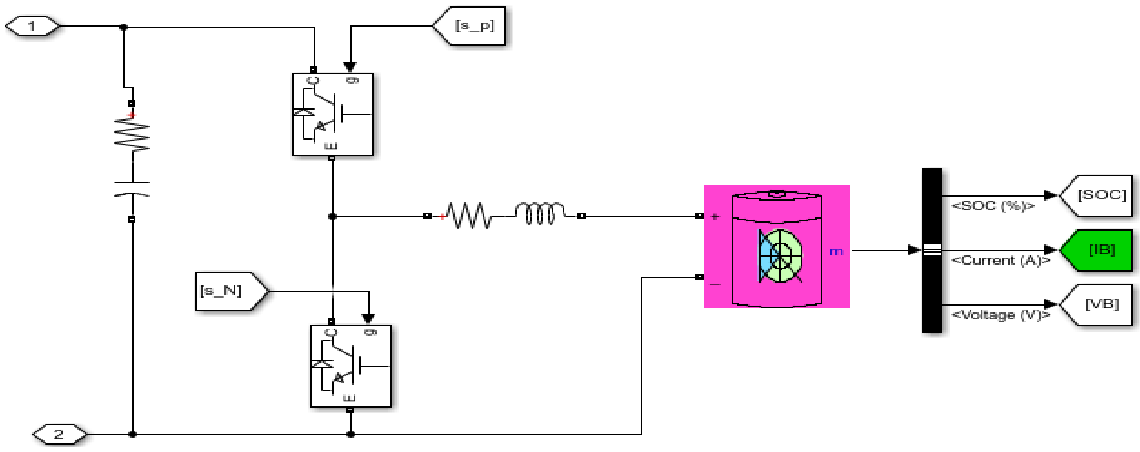

Figure 3.13. Modeling of battery with bi-directional DC to DC converter

This microgrid system uses IGBT/diode as the switching device in the circuit [57]. The main function of the bi-directional converter is to keep the system voltage at a certain reference value during charging or discharging.

The bidirectional converter contains two choppers (IGBT) connected to the circuit. They work in a complementary way, when one IGBT is on, the other IGBT is off [58]. This converter configuration can provide positive or negative current to the battery charging or discharging battery, respectively; however, the voltage level is positive.

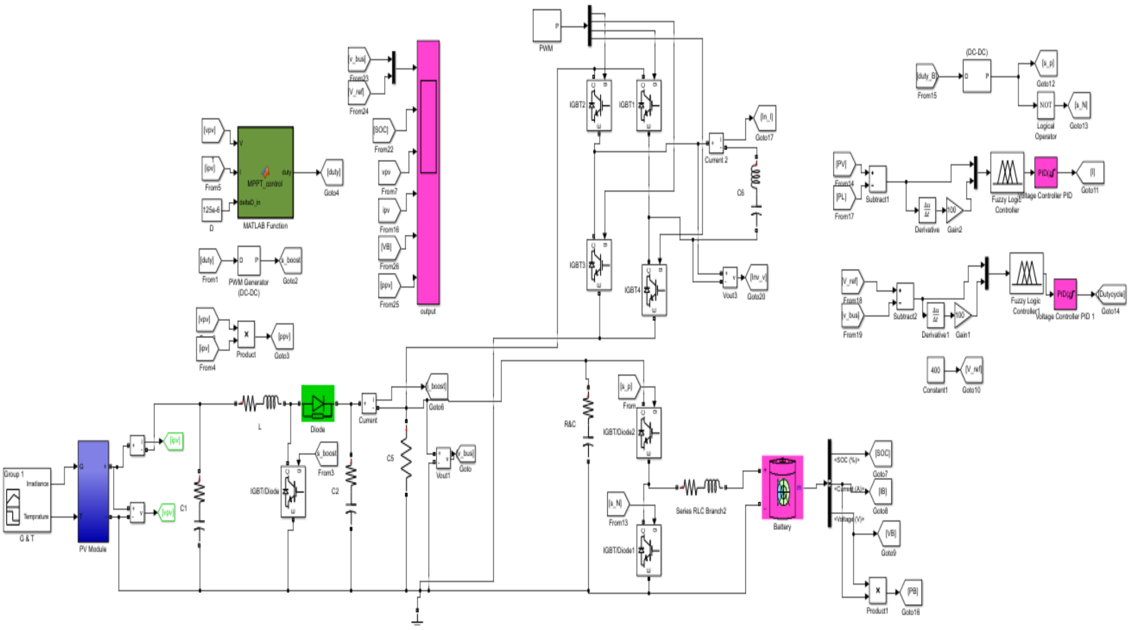

Figure 3.14. Overall modeling of microgrid energy management system

3.9. Controller for Microgrid Energy Management of the Standalone PV system.

3.9.1. Maximum Power Point Tracking Using Perturb and Observe Algorithm Controller for PV Management System

The basic MPPT structure used by the photovoltaic system perturbation and observation controller has two inputs, namely voltage and current, and the output is duty cycle. In this paper, the microgrid power system is controlled by a fuzzy, and fuzzy-PID controller, which is described as follows:

3.9.2. Fuzzy Logic Controller

Fuzzy logic control can detect sudden changes and heuristic variables, which is very good for microgrid power control and management systems. FLC is fast, robust, and follows input changes. It does not require prior knowledge of the system and uses simple mathematics. [29]. Fuzzy logic controllers are suitable for photovoltaic systems that are characterized by non-linearity, input variations.

To define a fuzzy set, both the members of the set (values) and the degree of membership are needed. Fuzzy logic operations are used to relate fuzzy sets. The fuzzy logic controller is characterized by membership functions and fuzzy rules.

Fuzzy input and output variables are represented by membership functions (MF). Also in fuzzy rules, the Mamdani fuzzy is the most used fuzzy membership rule set in this thesis work.

3.9.3. Fuzzy Logic Based Battery Management System

The battery management system adjusts the power flow in the microgrid system to meet the load demand. In this paper, a functional battery is used as an energy storage device. In addition, in order to obtain the required SOC, the fuzzy logic controller is designed to charge or dischage mode. The inputs of the fuzzy logic controller are ΔP and ΔSOC, and the output variable is current.

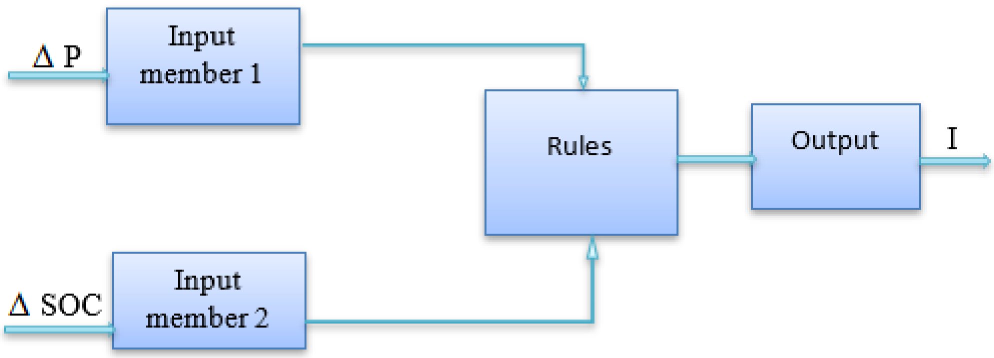

Figure 3.15. Fuzzy logic controller block diagram

The input and output variables used in the fuzzy logic controller are determined. In the work of this thesis, the fuzzy logic controller has a dual input variable and a single output system. The parameters and rules are described in the control algorithm. The basis of the FLC rule is based on the difference in power and the change of the state of charge, and the control output is the current. The change in power and the change in state of charge are calculated using the following formula:

$$\Delta P = P_{pv} - PL \tag{3.46}$$

$$\Delta SOC = SOC_{present} - SOC_{new} \tag{3.47}$$

The control is applied by controlling the power and current input of the battery [49]. The power, state of charge, and output are categorized into different regions which are negative, positive, and zero regions. Also, each region has sub-regions such as Negative Small (NS), Negative Big, (NB), Positive Big (PB), Zero (Z), and Positive Small (PS). Each input variable has members function of fuzzy set and it obtains 25 possible rules. These rules are described in Table 3.7.

Table 3.7. Rule base for fuzzy logic controller for battery management system.

Current		Δ P				
		NB	NS	Z	PS	PB
Δ SOC	NB	PB	PB	PB	PB	PB
	NS	PB	PB	PS	PS	PB
	Z	Z	Z	Z	PS	PB
	PS	NS	NS	NS	NS	PB
	PB	NB	NB	NB	NB	PB

Table 3.7 shows the fuzzy logic control rules of the microgrid battery management system. For example, when the power input variable is NB and the change in state of charge is NB, the output current is PB.

If the power is negative, the power generation system does not provide enough power to meet the load demand and the fuzzy logic controller is forced to discharge the battery to meet the load demand. If the state of charge is greater than the current state of charge, the change in the state of charge is negative and the battery should operate in discharge mode. The input variables, change of state of charge, change of power and control of current output of FLC are shown in Figure 3.16 to 3.18.

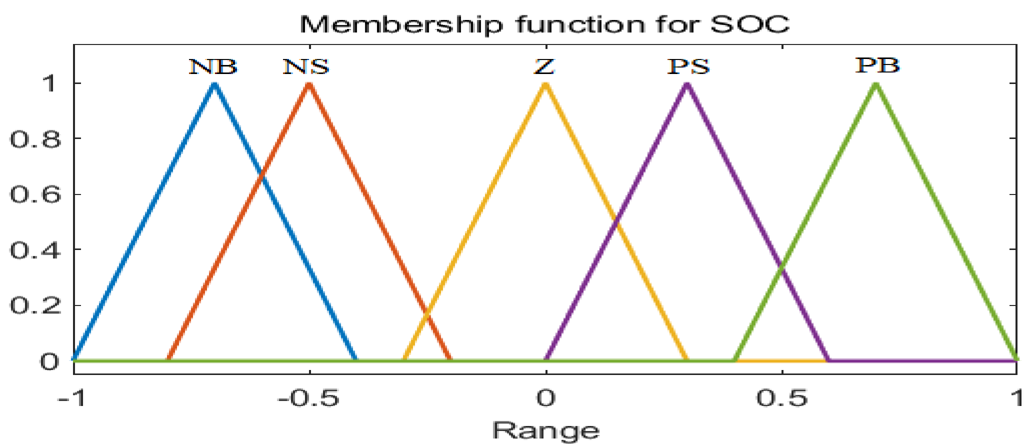

Figure 3.16. FLC input membership function SOC for battery management system

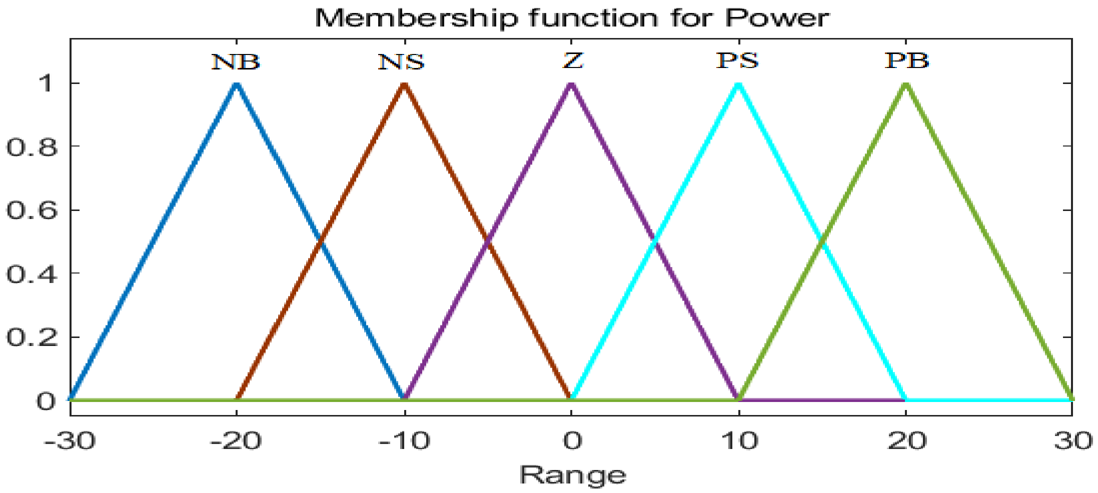

Figure 3.17. FLC input membership function power for battery management system

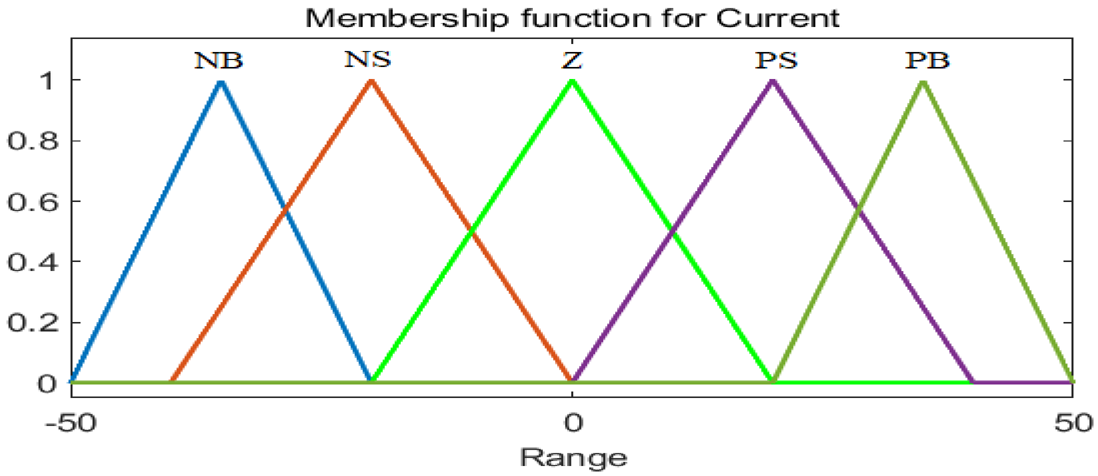

Figure 3.18. FLC output membership function current for battery management system

3.9.4. Fuzzy-PID Controller

The combination of these two controller structures is one of the best ways to control the output voltage of the system. In this thesis work, the fuzzy- PID controller is used to control the overall microgrid system and the charge and discharge operation of the battery. Using a fuzzy-PID controller utilizes both the operation of the fuzzy controller and the simplicity of the PID controllers at the same time [29], and [59]. Figure 3.19 shows the fuzzy-PID controller.

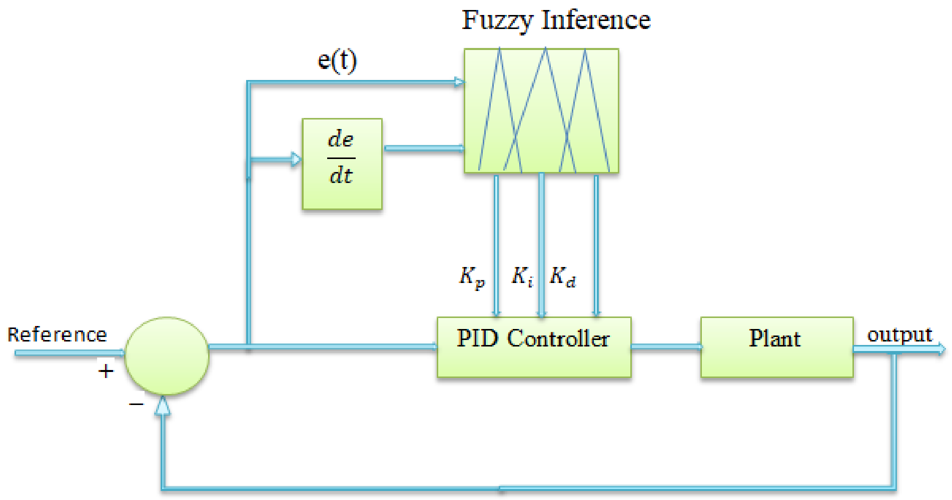

Figure 3.19. Block diagram of Fuzzy-PID controller [76].

3.9.5. Fuzzy-PID Controller for DC-link Voltage Controller

The input and output variables used in the fuzzy-PID controller are determined. In this thesis work, the fuzzy-PID controller has double input variables and a single output system. The fuzzy-PID controller takes the error and change in error as input and then the fuzzy logic rule forces to modify the parameters of K_p, K_i, and K_d are tuned online automatically. The parameters and rule base are described in the control algorithm. The rule base of the fuzzy-PID controller is based on the error (e) and change in error signal (Δe (n), and gain.

The error is the difference between the DC link output voltage and a reference voltage, and also the change in error is the difference between the current error and the old error. The error e(n) and change in error Δe(n) is calculated from the following Equations:

$$e(n) = V_{ref} - V_{out} \tag{3.48}$$

$$\Delta e(n) = e(n) - e(n-1) \tag{3.49}$$

The e (n), Δe (n), and output are categorized into different regions which are negative, positive, and zero regions. Each input variable has members function of fuzzy set, and it obtains 25 possible rules. These rules are described in Table 3.8.

Table 3.8. Rule base for fuzzy logic controller for DC link voltage

Output		Change in error				
		NB	NS	Z	PS	PB
Error	PB	Z	P	P	P	P
	PS	N	Z	P	P	P
	Z	N	N	Z	P	P
	NS	N	N	N	Z	P
	NB	N	N	N	N	Z

Where the parameters used in the rule are NB, NS, PS, PB, and Z are negative big, negative small, positive small, positive big, and zero respectively. Also, N, Z, and P are chosen for output which represents negative, zero, and positive respectively. In fuzzy-PID controller system, the applied rules are:

i. When the output voltage is much higher than the reference voltage, the controller must be very high, so that the DC link voltage approaches the value of the reference voltage.

ii. A small change of controller value is needed as the DC link of voltage is approaching the reference voltage.

iii. The controller must remain constant, when the output voltage of the system is near the reference voltage.

iv. The controller needs to be changed slightly to prevent the DC link voltage from deviating from the system reference voltage.

The input variables, error, change in error, and output controller of the fuzzy-PID controller are shown in Figures 3.20 - 3.24.

Fuzzy interface designer for DC link voltage controller

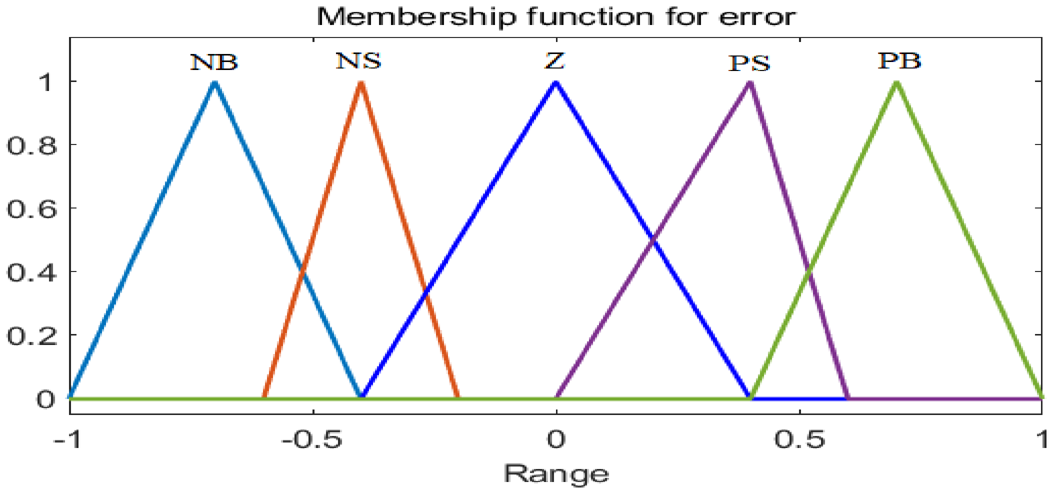

Figure 3.20. Input membership function error

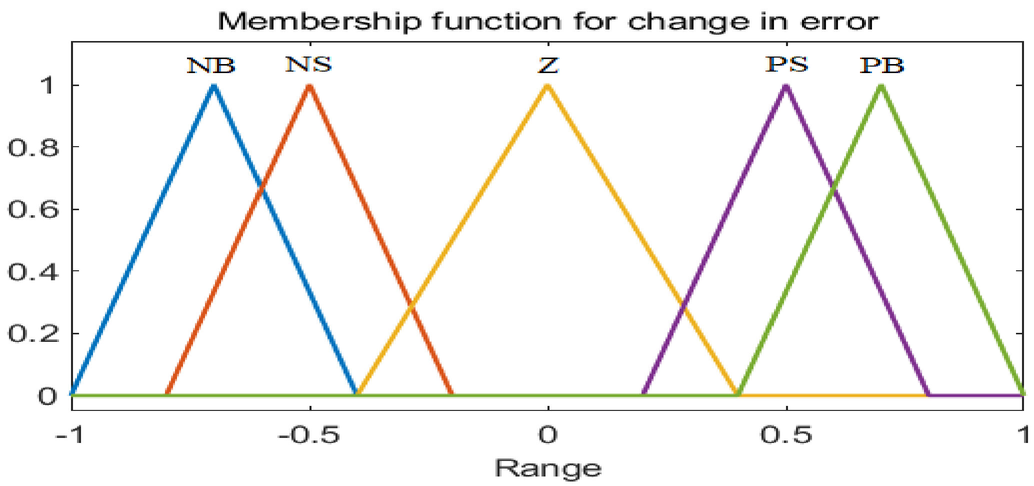

Figure 3.21. Input membership function change in error

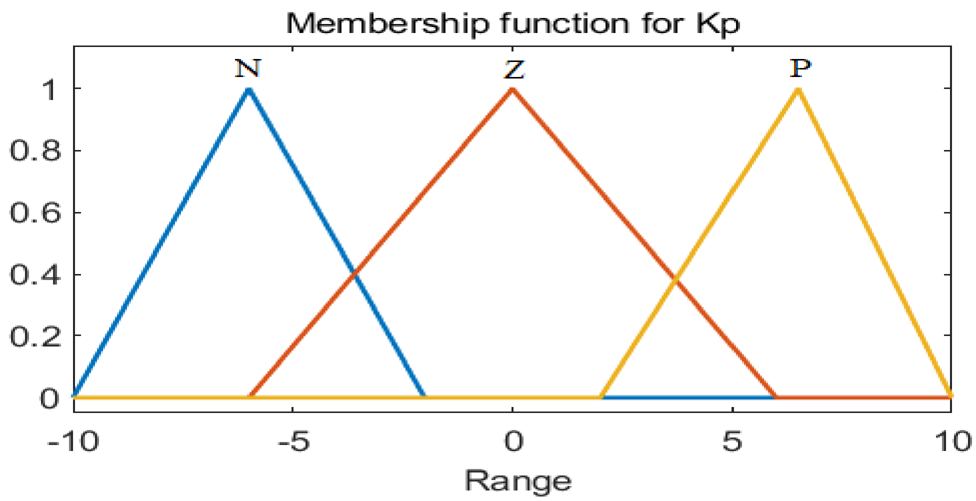

Figure 3.22. Output variable for fuzzy-PID controller

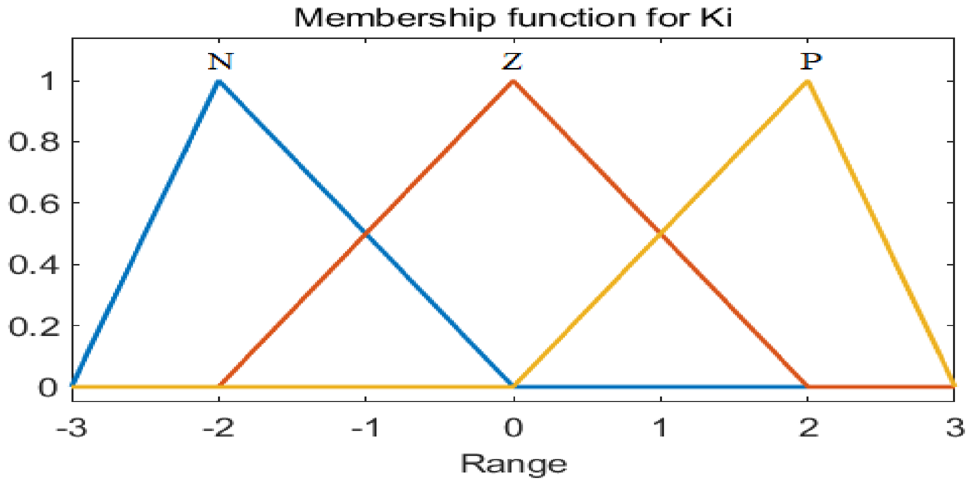

Figure 3.23. Output variable for fuzzy-PID controller

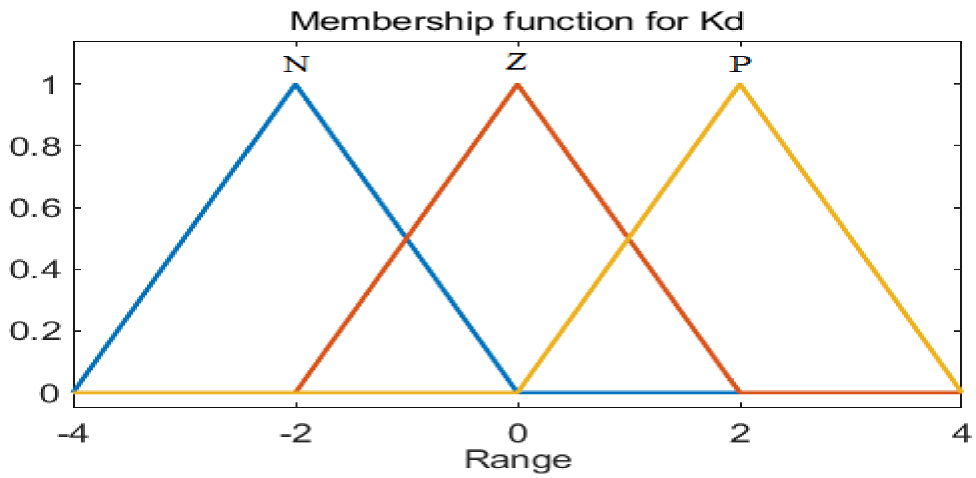

Figure 3.24. Output variable for fuzzy-PID controller

CHAPTER FOUR

RESULTS AND DISCUSSIONS

This chapter presents the modeling and analysis of the microgrid energy management system and the control of standalone photovoltaic systems. The microgrid system is a compromise between photovoltaic solar energy and the boost converter, MPPT, battery, bidirectional converter and the inverter.

In addition, this chapter also summarizes the characteristics of the microgrid energy management system and its achievements in the ICT center of the Ambo University. The optimization is completed with the HOMER PRO software and the main tasks are: simulation, optimization and sensitivity analysis. During the optimization process, the performance of the microgrid component system was analyzed. Additionally, feasibility and energy costs were discussed.

4.1. MATLAB/Simulink Simulation Results

In this thesis work, the system is simulated under different atmospheric conditions with different solar radiation and temperature. During system simulation, there are some power fluctuations. Therefore, the proposed algorithm based on perturb and observer provides faster response by tracking the maximum power point under changing temperature and irradiance. The total output power of the photovoltaic array system is 70kW, which is realized by the MPPT algorithm based on O and P, providing the most efficient microgrid system. Therefore, the MPPT and fuzzy-PID controller used in the microgrid energy management system are used to control the voltage, current and photovoltaic power.

The power of photovoltaic array is directly related to the solar irradiance. However, the solar irradiance at night and early morning is very low. Therefore, the power of the photovoltaic array is reduced to zero. The time axis shows, how the value of a system variable has changed over some period of time, for each of simulation.

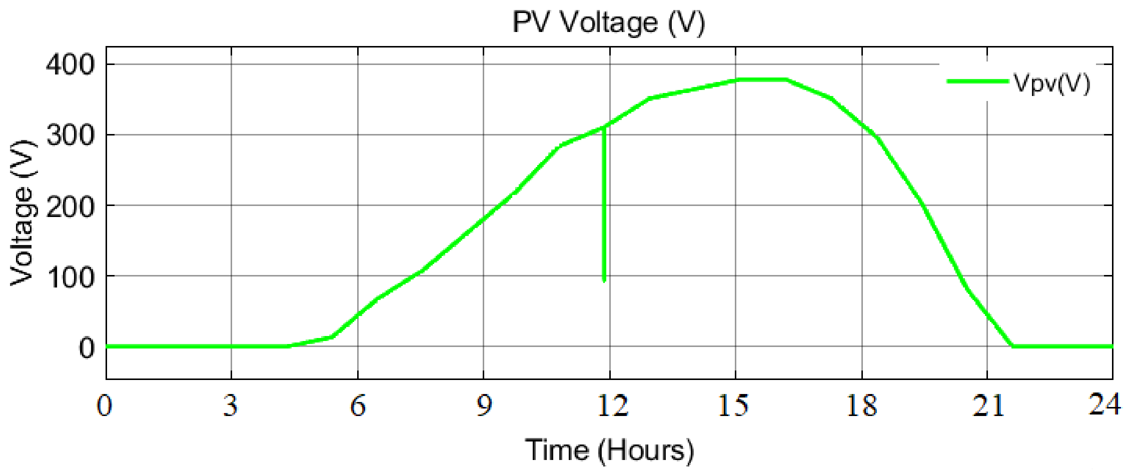

Figure 4.1. Output of photovoltaic voltage

As shown in the Figure 4.1, shows that with the increasing solar irradiance the output voltage is also increases, however, the solar irradiance has little effect on output voltage. Using maximum power point tracker, the maximum voltage is recorded from 14:00 to 16:00 hour. Also, at 11:30 hour the spikes are happened, due to switching on and off the MPPT controller and during charging and discharging battery.

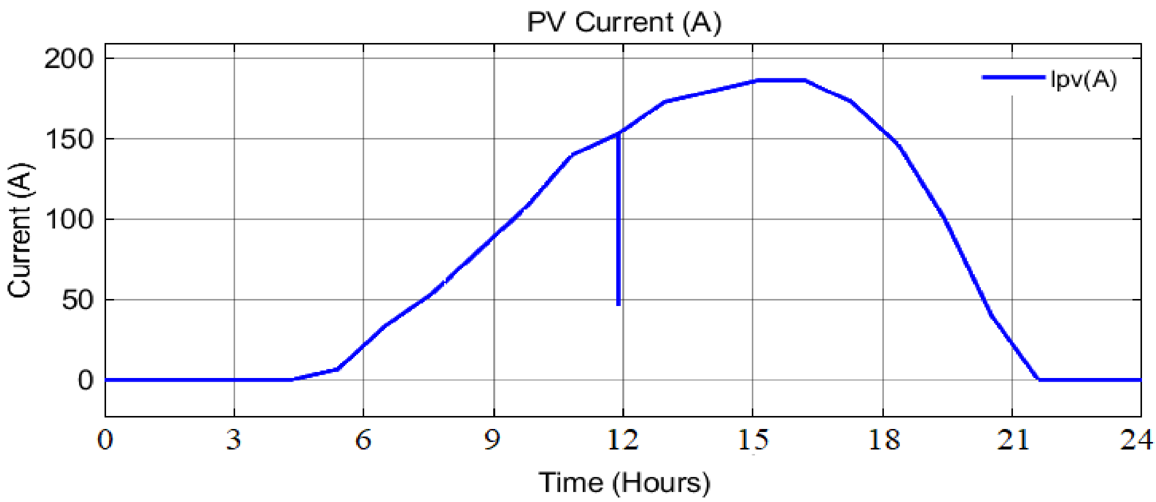

Figure 4.2. Output of photovoltaic current

Figure 4.2, shows that the higher the irradiance, the greater the output current. Solar irradiance with output current is directly relationship, which means when solar irradiance increases the output current increases. The maximum current is recorded from 14:00 to 16:00 hour, and when solar irradiance decreases the output current is also decrease that is when there is high clouds cover, high dust, and high air pollution, especially during night and early morning.

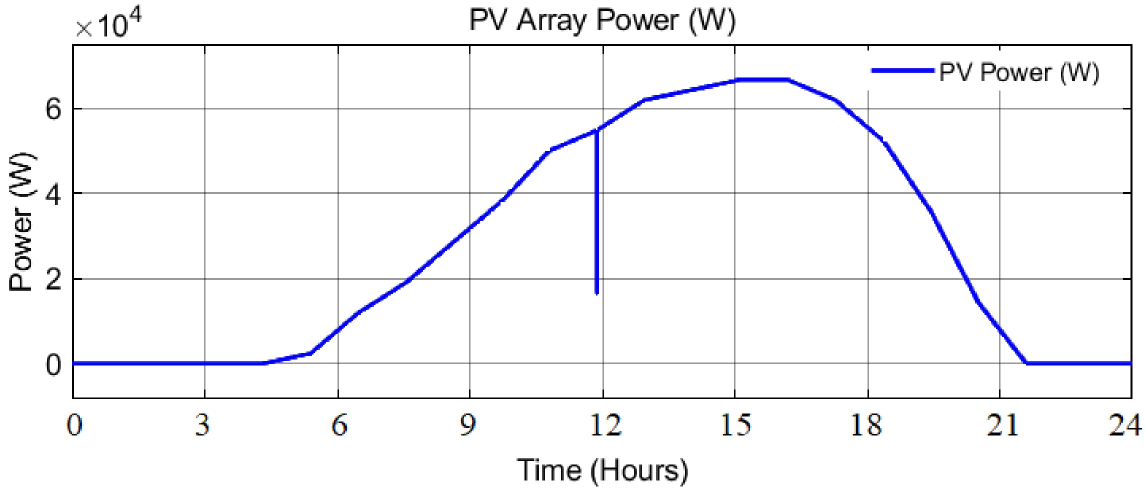

Figure 4.3. The output of photovoltaic power

Figure 4.3, shows that based on simulation results above, the PV maximum power generation is change with the irradiance. The power generation decreases with decreasing irradiance and increases with increasing irradiance. The maximum power is recorded at 15:00 hour. PV maximum power generation can be achieved at different irradiance with the utilization of P&O MPPT controller.

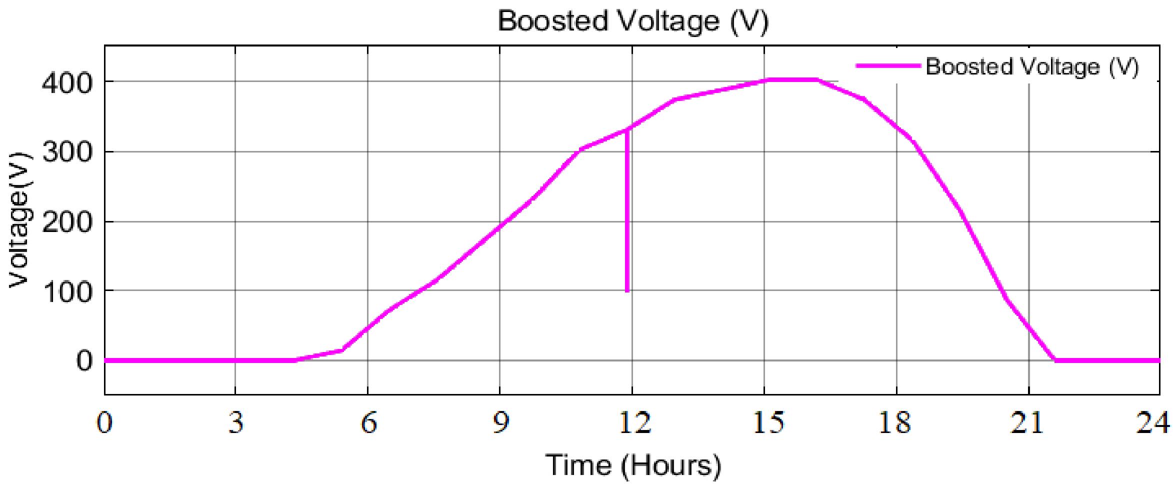

Figure 4.4. Boosted output voltage

As shown in Figure 4.4, in the detailed model of the photovoltaic array, the boost converter increases the DC voltage from 369.8 V to 400 V. By using Perturb and Observe method, under maximum point tracker the duty cycle of DC/DC boost converter is applied. The output voltage of the photovoltaic array is 369.8 V, but the voltage increases to 400V after using a boost converter.

Figure 4.5 shows the microgrid energy balance of photovoltaic arrays, batteries, and load demand under high solar irradiance. The PV power is coming to zero from 21:00 to 05:00 hours. During this period of high solar irradiance, the maximum photovoltaic power is generated. After 08:00 to 18:00 hours, the photovoltaic array generates power at the maximum power, which is sufficient to meet the load demand. Therefore, excess energy is transferred to the battery. Also, spikes are happened, due to switching on and off the MPPT controller.

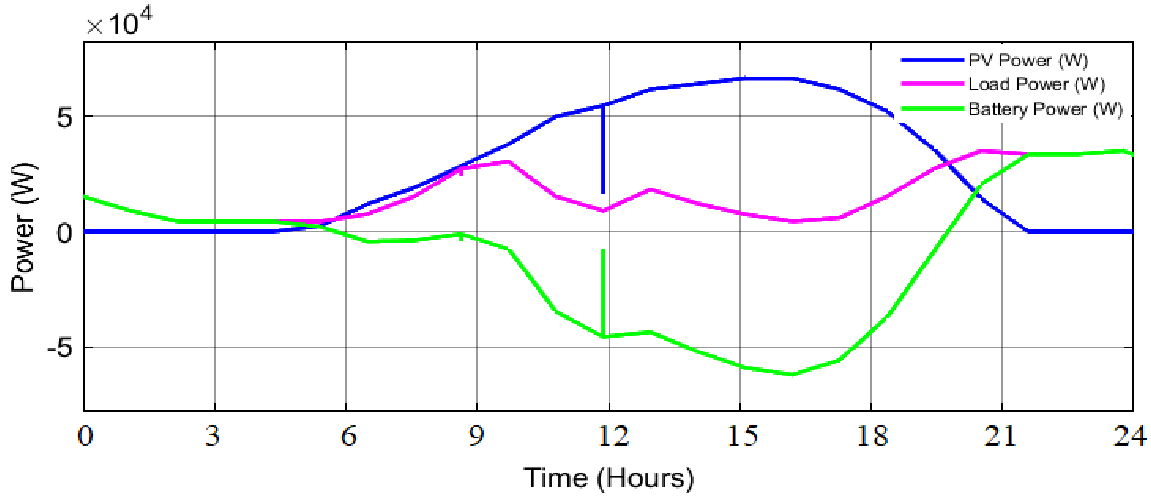

Figure 4.5. Microgrid energy balance of PV array with battery and load demand under high solar irradiance

Figure 4.6 shows the energy output of the photovoltaic array with low irradiance. The energy generated by the photovoltaic array during low irradiance is less than the energy generated by the photovoltaic array during high irradiance.

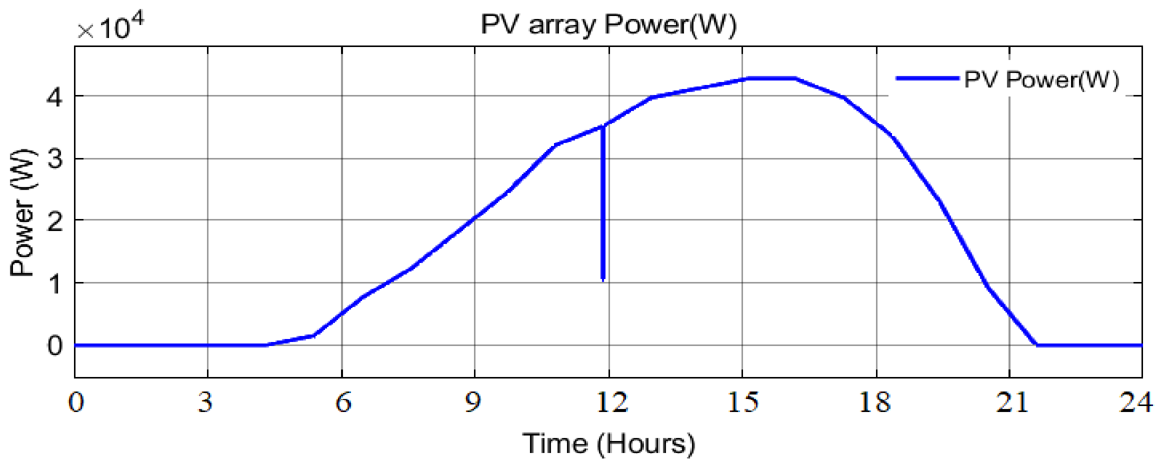

Figure 4.6. The output of PV array power under low irradiance

Figure 4.7 shows that the load demand changes from time to time. As shown in the figure, the maximum load of the system is 35kW, and the minimum load is 4.9kW at 20:30 hour and 02:00 hour respectively.

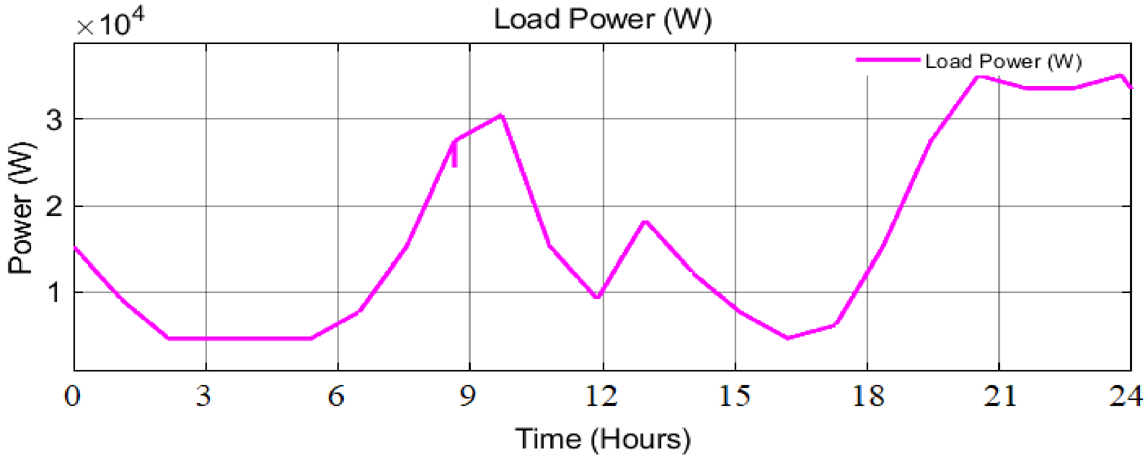

Figure 4.7. The output of load power

As shown in Figure 4.8, the battery is charging, when the load demand is less than the power generation capacity, and the battery is discharging when the load demand is greater than the power generation capacity. As it can be shown from 10:00 to 19:00 hour the PV array power is greater than load demand, and from 00:00 to 10:00 hour and again from 19:00 to 24:00 hour the load demand is greater than PV array power, and the battery is charging and discharging respectively. In addition, as the battery is charged and discharged, the energy becomes positive and negative respectively.

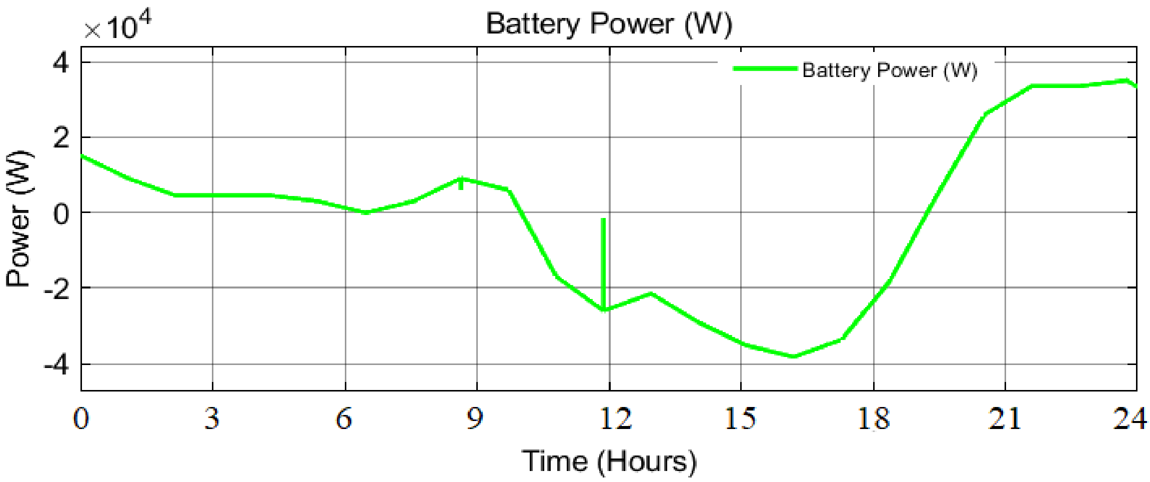

Figure 4.8. The Output of battery power

Figure 4.9 shows that from 21:00 to 5:00 hour the power of PV array is coming to 0 W. From 00:00 to 05:00, the battery supplies power to the load. After 05:00 hours the PV array starts producing energy; however, it was not sufficient to meet the load demand; so, batteries continued to supply power until 10:00 hour. Again from 10:00 to 19:00 hour the PV array power was enough to meet the load demand and, the batteries were charged. Also, from 19:00 to 22:00 hours, the batteries start again to help photovoltaic power by discharging. At 22:00 hour the PV array power was coming to zero, and the batteries started to fulfill load demand until 24:00 hour.

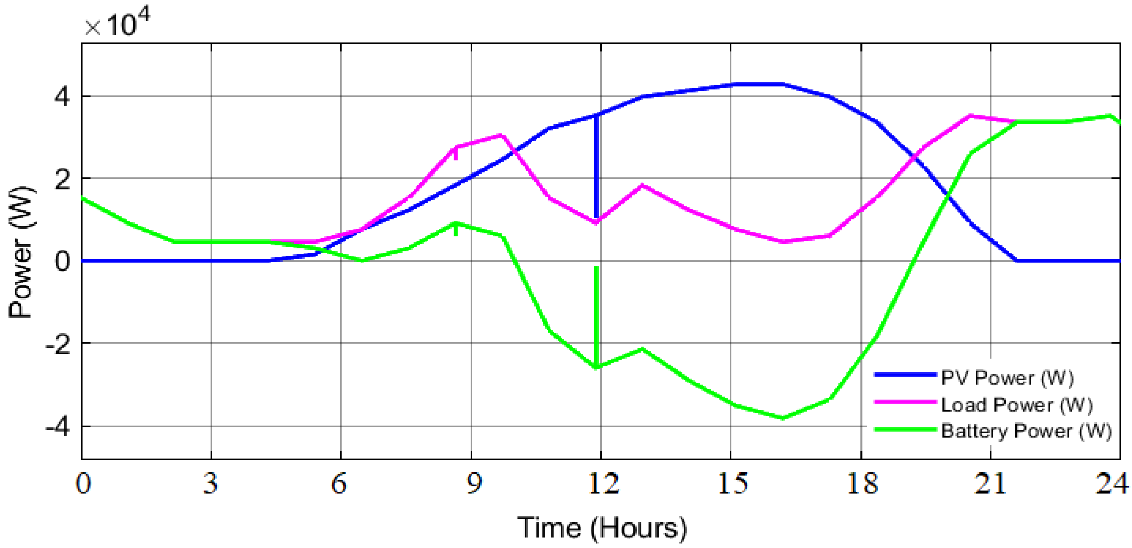

Figure 4.9. Microgrid energy balance of PV with battery and load demand under low solar irradiance.

Figure 4.10 shows that the charging and discharging modes. Therefore, the battery is in charging mode, because the PV array system is generating enough power and the state of charge is increasing. In addition, when the photovoltaic array does not generate enough energy, the battery discharges and the state of charge decreases.

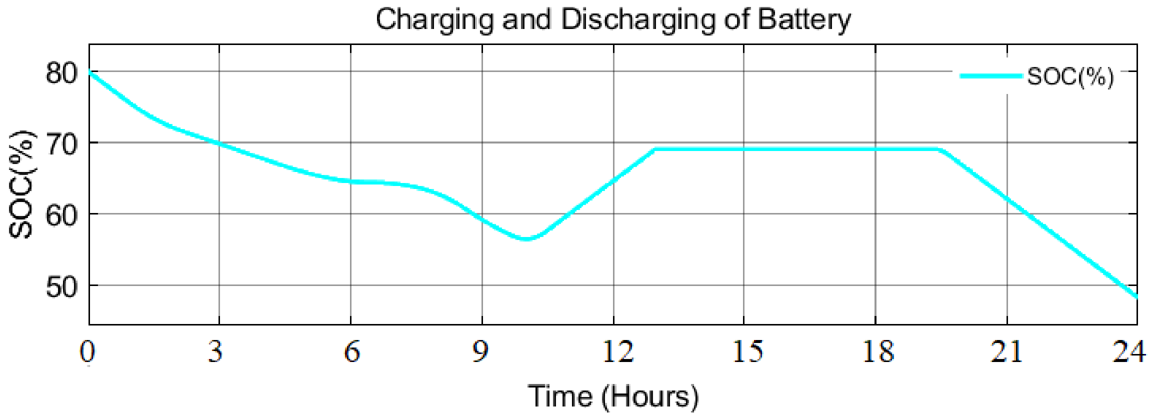

Figure 4.10. Simulation results of charging and discharging mode

Figure 4.11 shows the use of a fuzzy-PID controller to maintain the DC link voltage at the reference value. In addition, the DC link voltage follows the reference voltage with good accuracy and stability. Therefore, regardless of whether the energy storage is charging or discharging, the DC bus voltage must be stable and remain unchanged, during the entire operation. In the fuzzy-PID controller, the system rise time is short, the oscillation is small, and the voltage fluctuation is small.

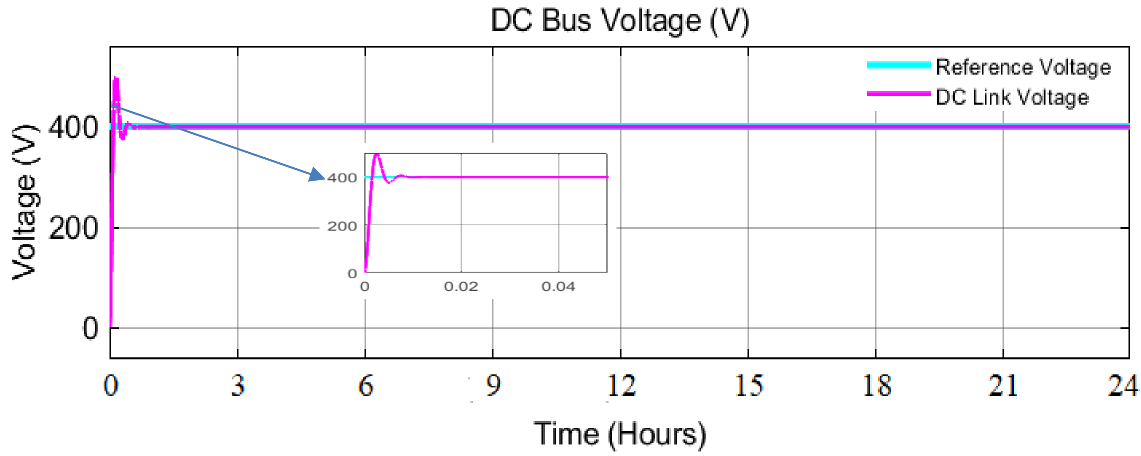

Figure 4.11. DC bus voltage with fuzzy-PID controller

Figure 4.12 shows the error between the reference voltage and the DC link voltage using the fuzzy-PID controller. As shown in the figure 4.12, the error is close to zero, which means that the DC link voltage tracks the reference voltage for up to 24 hours of simulation time. In general, the fuzzy-PID control system is also very stable and performs well.

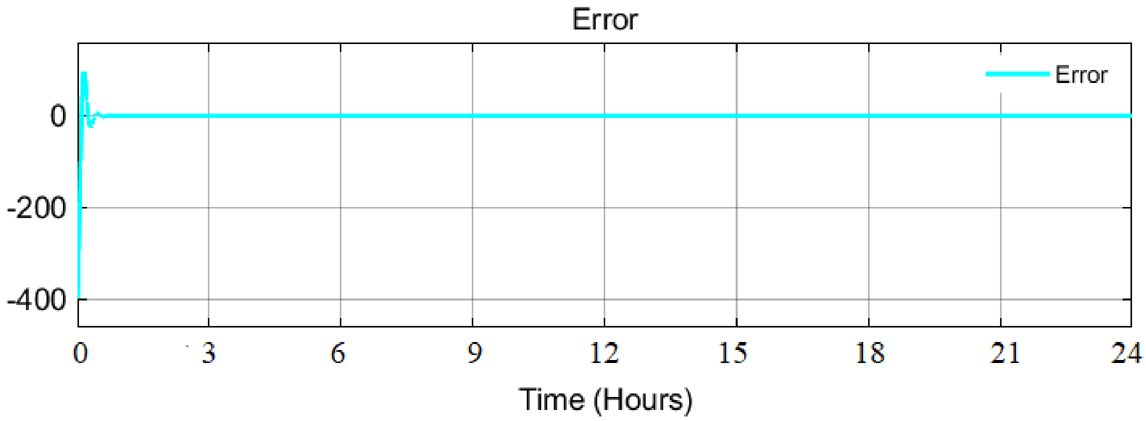

Figure 4.12. Voltage error of DC-link voltage using a fuzzy-PID controller

The microgrid photovoltaic array system provides DC power, but there is an AC load. To supply power to the AC load, an inverter is used in the system. As shown in Figure 4.13, an IGBT (Insulated Gate Bipolar Transistor) based inverter is used to convert DC power to AC power. It shows that the efficiency of the inverter is less harmonic distortion, which shows that it has the ability to convert DC to AC with accurate waveforms. This waveform has a two-level signal, which is a voltage that oscillates between a positive voltage and a negative voltage.

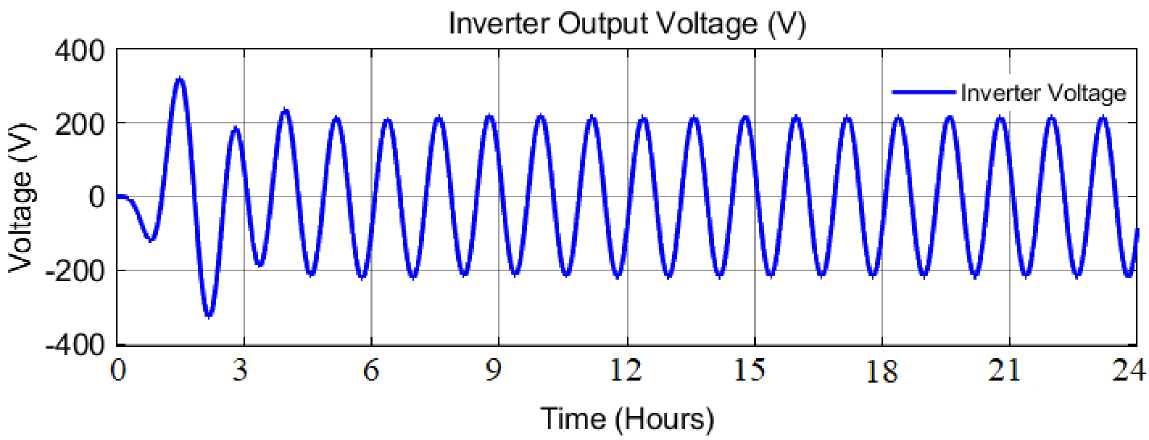

Figure 4.13. Single-phase inverter output voltage.

4.2. HOMER PRO Simulation Results

The output of the simulation contains different combinations for each component and offers a list of feasible schemes depends on the values of the net present cost and cost of energy. The optimization result for this thesis has two main groups which are called categorized results & overall optimization results. The overall optimization results for Ambo University ICT center building were shown in Appendix C.

The sequential optimization cost is simulated from lowest cost to highest cost. From calculation the net present cost is 346,323.32$ and cost of energy is $0.349/kWh. However, using HOMER PRO software, the sequential optimization cost is simulated from lowest cost to highest cost, the present net cost and the cost of energy were $291,359 and $0.309/kWh, respectively. It is necessary for the microgrid standalone PV system of the ICT center, due to its greater reliability and efficiency and shown in Appendix C.

The cost of the proposed for this standalone microgrid energy system is higher than the cost set by the Ethiopian electric utility company. However, this may be an acceptable alternative, because of its efficiency, reliability, and other areas where power is not available. In addition, the price is free from interruption and fuel cost.

CHAPTER FIVE

CONCLUSIONS AND RECOMMENDATIONS

5.1. Conclusions

This paper analyzes the microgrid energy management control system and the photovoltaic system composed of photovoltaic arrays, batteries and power electronic equipment to meet the needs of the community.

Various significant aspects of the microgrid system, such as sizing, modeling, optimization, analysis of system components, photovoltaic system management, and battery management, were discussed. Also, the bi-directional converter is used to manage the power flow between the DC bus and the battery through the DC link voltage. It has been proposed the MATLAB/Simulink to perform the microgrid system modeling and analysis for standalone solar photovoltaic systems. The photovoltaic array, O and P with MPPT, bidirectional converter, and inverter has been described.

The photovoltaic array generates maximum power, which is achieved by using perturbation and observation methods to extract maximum power point tracking during high irradiance. However, during periods of low irradiance, the energy produced by the photovoltaic array is lower, so during this period the battery storage is considered.

Microgrid energy management provides: When the power demand is greater than the PV power generation, the battery discharges and provides additional power, and when the photovoltaic power generation is greater than the power demand, the battery charges. The battery is managed by the fuzzy logic controller, and the charging and discharging operation of the battery is analyzed. Also, battery charging and discharging are limited between 30% and 85% to extend battery life. The DC-link voltage is regulated at 400V by fuzzy-PID controller. Fuzzy-PID controller is applied to control, stabilize, manage the microgrid system, and minimize system error.

In addition, cost analysis was discussed using HOMER PRO software. The net present cost and the cost of energy were $291,359 and $0.309/kWh respectively which is, reliable and efficient. Generally, the standalone microgrid energy system is proposed by applying energy balance between energy generation and load demand, which can meet the problem of insufficient power access to the ICT center of Ambo University.

5.2. Recommendation

Energy is very important to accomplish different activities in human beings. Therefore, to improve energy crises, especially in Ambo University ICT center, the microgrid energy management standalone system contributed using a different controller.

This research was conducted for the Ambo University ICT center. For the actual implementation of the project, the selected area called Ambo University must take into account this research and update the system based on this work. The study area was randomly selected from the city of Ambo in the Oromia region, and it is not the entire Oromia region. In the future, researchers should study and investigate standalone microgrid energy photovoltaic systems in other areas with similar problems.

Finally, respective governments should participate in providing financial support for procurement, installation of the PV system, encourage the use of microgrid energy management PV solar energy, and propagate this energy solution for a clinic, commercial, and buildings.

REFERENCES

[1] B. A. Taye, "Design, modeling and control of standalone photovoltaic system for rural electrification in Ethiopia using MATLAB," *IJETT,* Vols. vol-66, p. 3, 2018.

[2] N. A. Luu, "Control and management strategies for a microgrid," NNT, University of Grenoble, 2014.

[3] M. Barbero, "Sizing and scheduling of a microgrid connected to the grid with integration of EV," ETSEIB, July 2017.

[4] P. Shaw, "Modeling and control of a battery connected standalone photovoltaic system," in *EENITR*, 2015.

[5] "[https://customenergy.com Most popular types of solar panels explained," [Online]. [Accessed 11 02 2021].

[6] "http://www.energybc.ca/cache/solarpv/www.cetonline.org/Renewables/PV," [Online]. [Accessed 11 02 2021].

[7] D. R. E. Matagne, "Optimization of photovoltaic power systems", London Dordrecht Heidelberg, New York: ISSN, 2012.

[8] S. Joshi, "Design of small scale solar powered house," in *G. H. Patel College of Engineering & Technology*, India, 2017.

[9] M. Taheruzzaman, "Design, planning, and modeling of renewable energy integrated microgrid for rural electrification in Bangladesh," in *MEAIE*, Germany, 2016.

[10] B. V. Emmanuel, "Solar PV system sizing," University Of Nairobi, 2009.

[11] P. S. Shimi Sudha Letha, "Bidirectional dc to dc converters: An overview of various topologies,switching schemes and control techniques," *IJET,* vol. 7, pp. 360-365, 2018.

[12] "https://en.wikipedia.org/wiki/Power_inverter," [Online]. [Accessed 11 02 2021].

[13] J. Grant, "Design and simulation of a DC microgrid for a small Island in Belize," Sustainable Energy Engineering – Iceland School of Energy, 2018.

[14] F. O. C. Edeko, "Design and implementation of solar charge controller with variable output," *JEE,* Vols. Vol 12, No 2, p. 1118 – 5058, 2015.

[15] L. W. Z. Irwanto M, "Photovoltaic powered DC-DC boost converter based on PID controller for battery charging system," *IOP*, 2020.

[16] N. S. S. Fawaz S. Abdullah, "Design and implementation of photovoltaic maximum power point tracking controller," *Journal of University of Babylon, Engineering Sciences,* Vols. Vol.(26), No.(5), pp. 135-146, 2018.

[17] Y. D. bhishek Kumar, "Energy management system controller for a rural microgrid," *RPG,* vol. 13, p. pp. 834–839, 2017.

[18] A. F. mjad Ali, "A review: DC microgrid control and energy management system," *IJEES,* Vols. Vol. 2, No. 2, pp. pp. 24-30, 2015.

[19] R. ,. D Anitha, "Energy management of a DC microgrid with hybrid energy sources," *IJPAM,* vol. Volume 118 No. 19, pp. 2631-2645, 2018.

[20] H. J. J. L. G. Ye Zhang, "Energy management strategy of islanded microgrid based on power flow control," *IEEE,* 2011.

[21] M. G. S. Sudipta Chakraborty, "Powere electronics for eenewable and distributed energy systems", Springer-Verlag Londo, 2013.

[22] D. G. Michaelson, "Predictive energymanagement of islanded microgrids with photovoltaics and energy storage," The University of Western Ontario, 2017.

[23] B. A. Taye, "Design, Modeling and control of standalone photovoltaic system for rural electrification in Ethiopia using MATLAB," *IJETT*, vol. 66, 2018..

[24] P. K. Vipul Narad, "Design and simulation of solar PV DC microgrid for rural Electrification," *IRJET*, vol. 06, no. 03, 2019.

[25] S. W. P. H. J. Kitson, "Modeling of an expandable, reconfigurable, renewable DC microgrid for off-grid communities," in *Energy*, 2019.

[26] M. B. Kumar, "Modeling and control of PV/wind," Halmstad Universty, 2017.

[27] H. A. Alharkan, "A control algorithm for the solar village microgrid system," in *Masters Theses*, 2016.

[28] Y. D. Abhishek Kumar, "Energy management system controller for a rural microgrid," *The Journal of Engineering,* 2017.

[29] Z. Almukhtar, "Fuzzy logic control for standalone photovoltaic energy conversion system, and innovation in renewable energy," Saint Mary’s University, Halifax, Nova Scotia, 2016.

[30] H. M. Mohammad Aman Yaqobi, "Control and Energy Management Strategy of Standalone DC Microgrid Cluster using PV and Battery Storage for Rural Application," *IJPER*, Vols. Vol. 2, No. 4, p. 53, 2018.

[31] M. T. Y. Sawle, "Design, analysis and optimal sizing of standalone PV/diesel/battery hybrid energy system using HOMER," in *Materials Science and Engineering*, 2020.

[32] D. A. R. y. m. K Pooja, "Bidirectional DC-DC converter for solar battery backup applications," *IEEE*, Vols. Vol. 06,, no. 02, pp. pp. 47-52, 2020.

[33] S. D. Gon, "Design of a standalone photovoltaic system for a typical household around Dessie City-Ethiopia," *AJEEE*, Vols. Vol. 7, No. 1, 1-7, 2019.

[34] N. M. A. Hanaa Mohamed Farghally, "Design and optimization of standalone photovoltaic system based on MPPT FLC controller for electric bikes charging station," *IJEE,* Vols. Volume 9, Number 2, pp. pp. 171-194, 2016.

[35] S. D. Gont, "Design of a standalone photovoltaic system for a typical household around Dessie City-Ethiopia," *American Journal of Electrical and Electronic Engineering,* Vols. Vol. 7, No. 1, 1-7, 2019.

[36] S. A. S. Uboori, "Standalone photovoltaic system," *Energy Sci. & Tech.*, vol. vol.6, 2016.

[37] T. K. Radu-Emil Precup, "Solar photovoltaic power plants", Springer, 2019.

[38] I. Z. M. N. Mohd Shawal Jadin, "A Sizing tool for PV standalone system," *JEAS*, Vols. Vol. 10, No. 22, pp. pp 1819-6608, 2015.

[39] T. M. Parimita Mohanty, "Solar photovoltaic system applications", Springer International Publishing Switzerland, 2016.

[40] M. A. E. T. El Shenawy, "Design and optimization of standalone PV system for Egyptian rural communities," *IJAER,* Vols. Volume 12, Number 20, pp. pp. 10433-10446, (2017).

[41] "https://www.alibaba.com/showroom/12v-200ah-deep-cycle-battery.html," [Online]. [Accessed 09 09 2021].

[42] "https://www.homeadvisor.com/cost/heating-and-cooling/solar-panel-prices," [Online]. [Accessed 09 09 2021].

[43] Y. S. Mohammed Kharrich and Mohamed Akherraz, "Optimal sizing of an islanded microgrid based on PV, wind and battery energy storage system," *International*

Conference on Automation, Control Engineering and Computer Science, vol. Vol.20, pp. pp.71 - 76, 2017.

[44] J. A. A. Emmanuel Kwaku Anto, "PID-based P&O MPPT controller for offgrid solar PV systems using Ziegler-Nichols tuning method to step, ramp and impulse inputs," *Journal of Multidisciplinary Engineering Science Studies,* vol. Vol. 2, no. Issue 7, 2016.

[45] K. I. Mirza Mursalin Iqbal, "Design and simulation of a PV system with battery storage using bidirectional DC-DC converter using Matlab Simulink," *IJSTR,* Vols. OLUME 6,, no. ISSUE 07, pp. pp 2277-8616, JULY 2017.

[46] N. A. R. A. Omar, "Modeling of a maximum power point tracker for a stand-alone photovoltaic system using MATLAB/Simulink," *International Journal of Low-Carbon Technologie,* no. 9, p. pp 195–201, 2014.

[47] "https://www.google.com/search?q Solar panels specifications," [Online]. [Accessed 11 02 2021].

[48] B. Alsayid, "Modeling and simulation of photovoltaic Cell/module/array with two-diode model," *International Journal of Computer Technology and Electronics Engineering,* Vols. Volume 1,, no. Issue 3, June 2012.

[49] Y. Zhang, "Control and power management of photovoltaic systems with plug-in hybrid electric vehicles as energy storage," University of Tasmania, October 2017.

[50] J. Grant, "Design and simulation of a DC microgrid for a small Island in Belize," Sustainable Energy Engineering – Iceland School of Energy, 2018.

[51] Y. Ding, "Energy management strategy of PV grid-connected household nano-grid system," 2018.

[52] R. Ramachandran, "Energy management control for multimode microgrid renewable integration," West Virginia University, 2013.

[53] H. C. Bharath K R, "Control of bidirectional DC to DC converter in renewable based DC microgrid with improved voltage stability," *IJRER,* vol. Vol.8, no. No.2, June, 2018.

[54] Z. M. Karimi, "Modelling, implementation and performance analysis of hybrid wind-solar power generator with battery storage," Initiative Energy for Sustainability of the University of Coimbra, 2014.

[55] H. Deng, " Converters analysis and simulation in Microgrid," California State University, Sacramento, 2017.

[56] S. Sumaiya, "Modeling, designing, and analysis of a standalone PV DC microgrid system," in *MS thesis, GSU*, 2018.

[57] M. J. Rana, "Decentralized control of DC microgrids with energy storage systems," King fahd universty of petroleum and minerals dhahran, 2017.

[58] Y. F. Q. Michele Martino, "Intelligent control for distributed system," Department of Energy Technology-Pontoppidanstraede 101 Aalborg University, Denmark, 2012.

[59] Hussein, "Hybrid fuzzy-PID controller for buck-boost converter in solar energy-battery systems," Western Michigan University, 2015.

[60] S. Sumaiya, "Modeling, designing, and analysis of a standalone PV DC microgrid system," 2018.

[61] W. Bisschoff, "Design of an energy management system utilizing optimum energy consumption of a distribution level microgrid," Potchefstroom Campus of the North-West University, 2016.

[62] "[https://www.google.com/imgres the most common types of solar panel]," [Online]. [Accessed 11 02 2021].

[63] "https://core.ac.uk/download/pdf/61802295. DC to DC converter pdf," [Online]. [Accessed 11 02 2021].

[64] M. B. Kumar, " Modelling and Control of PV/Wind," Halmstad, 2017.

[65] M. Y. Ali, "Energy management system of a microgrid with distributed generation," University of Ontario Institute of Technology Oshawa, Ontario, Canada, 2019.

[66] A. B. Arjav Harjai, "Study mf maximum power point tracking techniques in a solar photovoltaic array," NITR, Orissa.

[67] D. J. Becker, "What is a microgrid ?," APEC, 2014.

[68] A. H. A. Berair, "Auto tuning of PID controller using particle swarm Optimization method for DC motor speed control," Sudan University of Science and Technology, Sep-2017.

[69] S. K. A. Khusaibi, "DC microgrid simulation and control," 2017.

[70] M. Martino, "Intelligent control for distributed system," 2012.

[71] H. M. Mohammad Aman Yaqobi, "Control and energy management strategy of standalone DC microgrid cluster using PV and battery storage for rural application," *IJPER,* Vols. Vol. 2, No. 4, p. 53, 2018.

[72] P. S. R. Muthukumar, "An overview of microgrid system," *ISSN,* Vols. Vol. 9, No. 22, 2015.

[73] D. K. Sharma, "Analysis of the effect of fill factor on the efficiency of solar PV system for improved design of MPPT," in *Department of Electronics & Comm. Engg,* Udaipur INDIA, 2014.

[74] S. Woldeyes, "Assessment of standalone solar photovoltaic power systems performance and reliability for rural electrification in Ethiopia"," AAU, 2018.

[75] "https://energyeducation.ca/encyclopedia/Photovoltaic_effect," [Online]. [Accessed 11 02 2021].

[76] "modeling, designing, and analysis of standalone PV DC microgrid System," Georgia Southern University, GA, USA, 2018.

[77] "Design, planning, and modeling of renewable energy integrated," *MEAIE,* 2016.

[78] G. D. Filipe Perez, "DC microGrids", Paris-Saclay University, Evry, France: IBISC, 2018.

[79] G. D. Filipe Perez, "DC microgrids", Evry, France: IBISC Laboratory, Paris Saclay University, 2018.

APPENDIX

APPENDIX A: Overall block diagram of microgrid energy management system

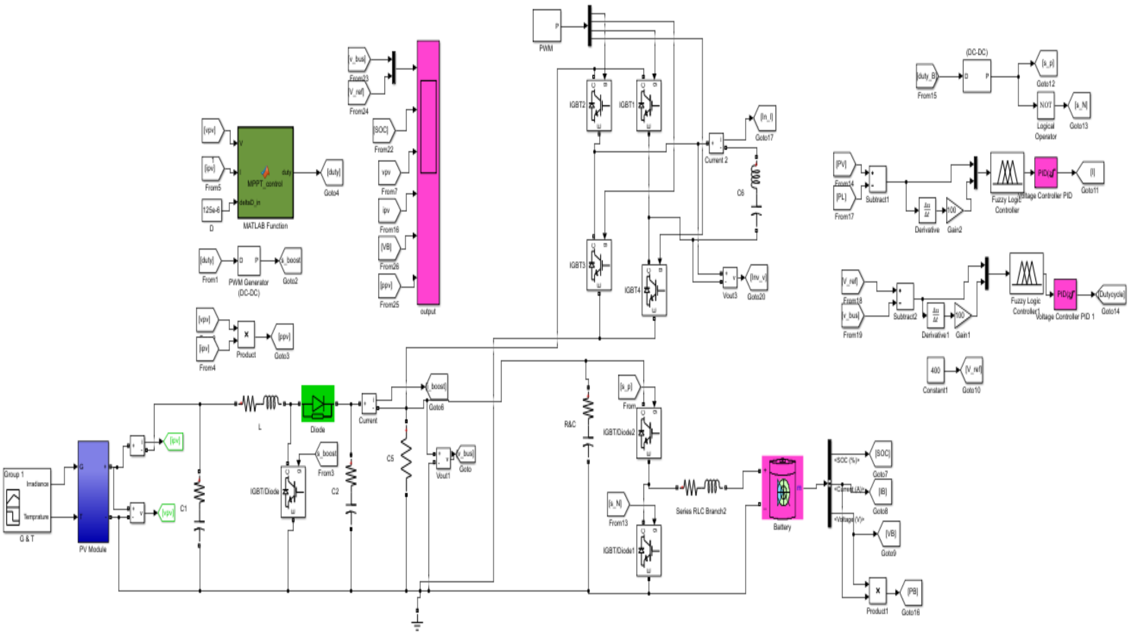

(a)

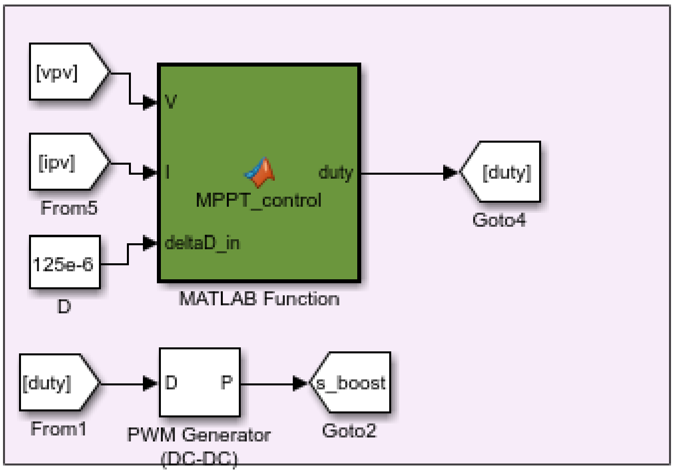

(b)

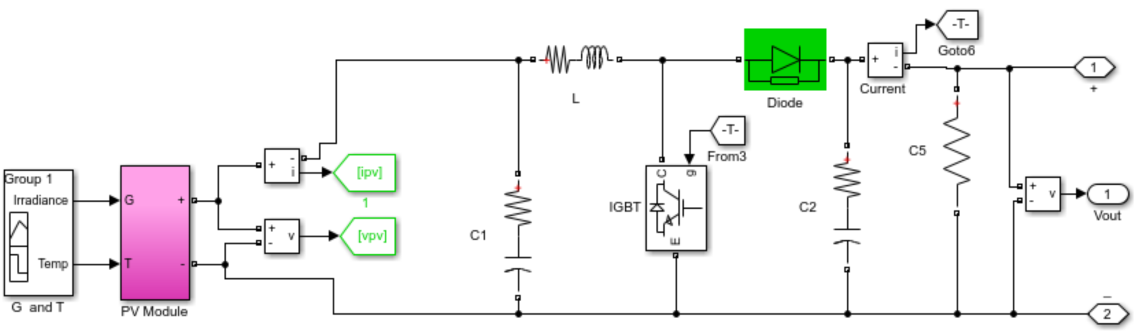

(c)

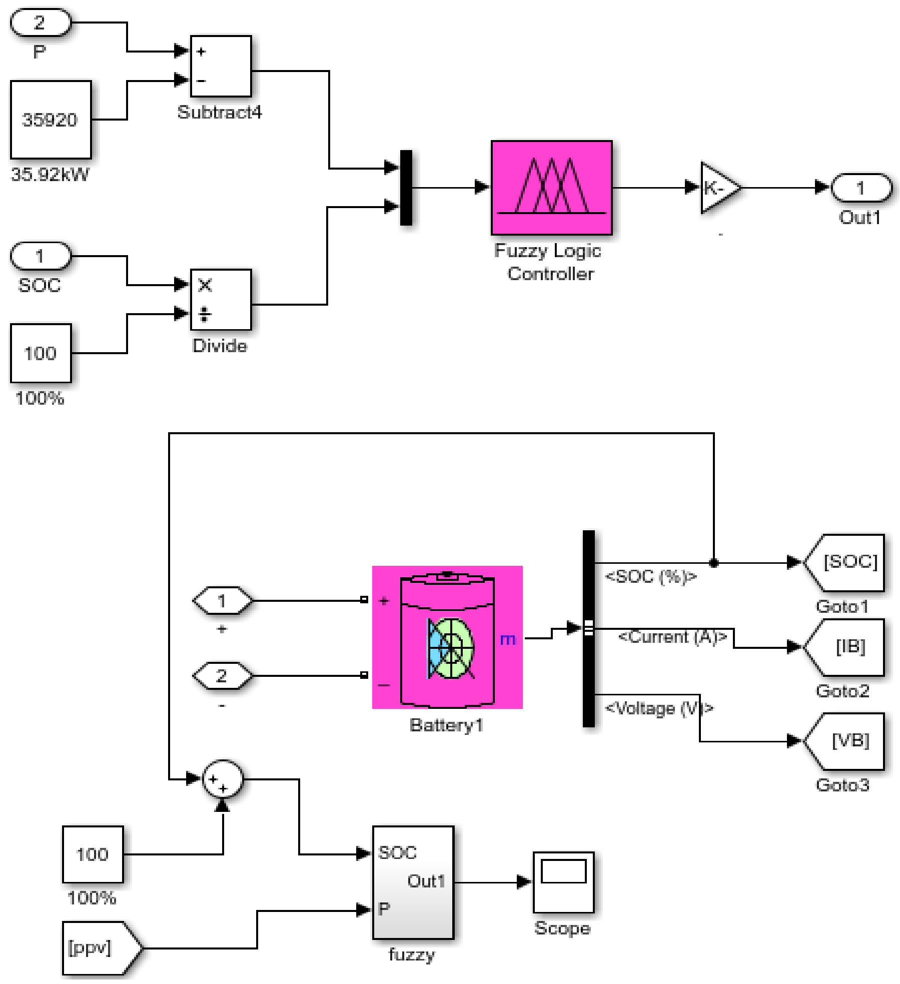

(d)

Figure A. 1 a) over all system b) PV control c) PV system d) battery control

APPENDIX B: Fuzzy rules

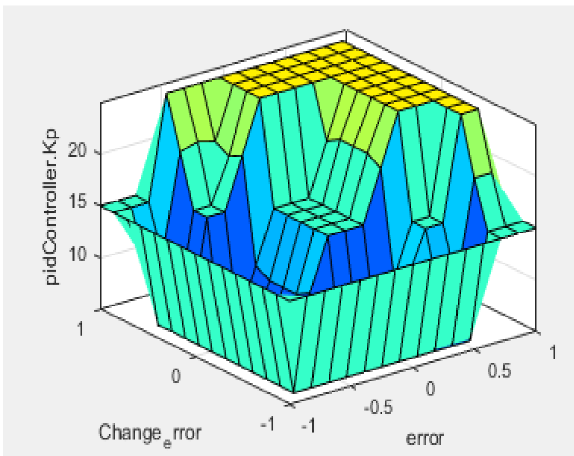

a)

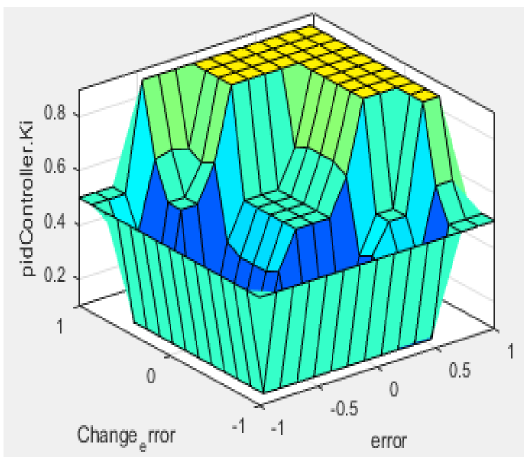

b)

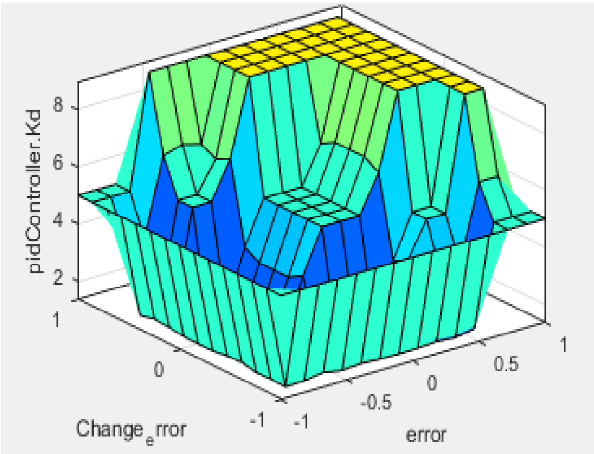

c)

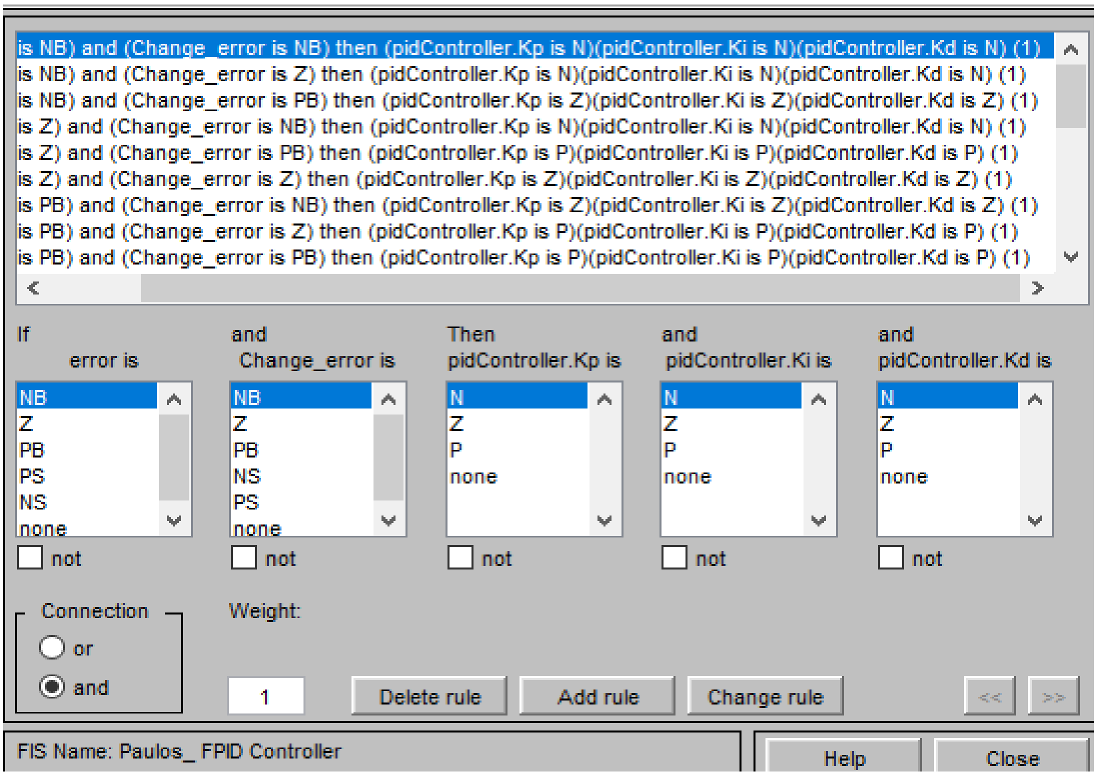

(d)

Figure B. 2 a) surface viewer of Kp, b) surface viewer of Ki, c) surface viewer of Kd, d) rule viewer

APPENDIX C: HOMER PRO simulation results

Export... Export All... **Sensitivity Cases** Compare Economics Column Choices...

Left Click on a sensitivity case to see its Optimization Results.

Sensitivity	Architecture								Cost				
battery time (years)					pv panel (kW)	battery	converter (kW)	Dispatch	COE ($)	NPC ($)	Operating cost ($/yr)	Initial capital ($)	O&M ($/yr)
10.0					70.0	335	35.7	CC	$0.329	$310,523	$7,220	$217,192	$4,361
20.0					70.0	335	35.9	CC	$0.309	$291,359	$5,727	$217,318	$4,364

(a)

Architecture								Cost				
				pv panel (kW)	battery	converter (kW)	Dispatch	COE ($)	NPC ($)	Operating cost ($/yr)	Initial capital ($)	O&M ($/yr)
				70.0	335	35.7	LF	$0.329	$310,523	$7,220	$217,192	$4,361
				70.0	335	35.7	CC	$0.329	$310,523	$7,220	$217,192	$4,361
				70.0	334	36.2	LF	$0.330	$310,945	$7,226	$217,526	$4,370
				70.0	334	36.2	CC	$0.330	$310,945	$7,226	$217,526	$4,370
				70.0	335	36.1	LF	$0.330	$310,996	$7,231	$217,523	$4,370
				70.0	335	36.1	CC	$0.330	$310,996	$7,231	$217,523	$4,370
				70.0	333	36.6	LF	$0.330	$311,239	$7,230	$217,773	$4,377
				70.0	333	36.6	CC	$0.330	$311,239	$7,230	$217,773	$4,377
				70.0	336	36.3	LF	$0.330	$311,313	$7,241	$217,706	$4,374
				70.0	336	36.3	CC	$0.330	$311,313	$7,241	$217,706	$4,374
				70.0	333	36.8	LF	$0.330	$311,368	$7,233	$217,863	$4,379
				70.0	333	36.8	CC	$0.330	$311,368	$7,233	$217,863	$4,379
				70.0	337	36.2	LF	$0.330	$311,390	$7,246	$217,720	$4,374
				70.0	337	36.2	CC	$0.330	$311,390	$7,246	$217,720	$4,374

(b)

Figure C. 2 a) overall optimization results, b) categorized results

APPENDIX D: Battery storage specification

DC12-200 (12V200Ah)

DC (Deep Cycle) series is specially designed for frequent cyclic discharge. By using strong grids and specially designed active material, the DC series battery offers 30% more cyclic life than the standby series. It is suitable for solar energy systems, marine and RV etc.

Specification

Cells Per Unit	6
Voltage Per Unit	12
Capacity	200Ah@10hr-rate to 1.80V per cell @25℃
Weight	Approx. 60.0 Kg (Tolerance±1.5%)
Max. Discharge Current	2000 A (5 sec)
Internal Resistance	Approx. 4 mΩ
Operating Temperature Range	Discharge: -20℃~60℃ Charge: 0℃~50℃ Storage: -20℃~60℃
Normal Operating Temperature Range	25℃±5℃
Float charging Voltage	13.6 to 13.8 VDC/unit Average at 25℃
Recommended Maximum Charging Current	60 A
Equalization and Cycle Service	14.6 to 14.8 VDC/unit Average at 25℃
Self Discharge	RITAR Valve Regulated Lead Acid (VRLA) batteries can be stored for more than 6 months at 25℃. Self-discharge ratio less than 3% per month at 25℃. Please charge batteries before using.
Terminal	Terminal F10
Container Material	A.B.S. UL94-HB, UL94-V0 Optional.

APPENDIX E: Solar module specification

250W Monocrystalline Solar Panels

ELECTRICAL SPECIFICATIONS

*STC : Irradiance 1000W/m^2, AM1.5 spectrum, module temperature 25°C

Model Type	CSS-MSP-250M-60
Peak power (Pmax)	250W
Cell Efficiency	17.24%
Maximum power voltage (Vmp)	30.8V
Maximum power current (Imp)	7.79A
Open circuit voltage (Voc)	37.4V
Short circuit current (Isc)	8.49A
Power Tolerance	±3%
Maximum system voltage	1000V
Series fuse rating (A)	15
Number of bypass diode	3/6